

# Accepted Manuscript

The Effect of Heavy Atom to Two Photon Absorption Properties and Intersystem Crossing Mechanism in Aza-Boron-Dipyrromethene Compounds

Ahmet Karatay, M. Ceren Miser, Xiaoneng Cui, Betül Küçüköz, Halil Yılmaz, Gökhan Sevinç, Elif Akhüseyin, Xueyan Wu, Mustafa Hayvali, H. Gul Yaglioglu, Jianzhang Zhao, Ayhan Elmali

PII: S0143-7208(15)00270-3

DOI: [10.1016/j.dyepig.2015.07.002](https://doi.org/10.1016/j.dyepig.2015.07.002)

Reference: DYPI 4842

To appear in: *Dyes and Pigments*

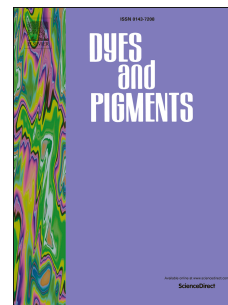
Received Date: 4 May 2015

Revised Date: 3 July 2015

Accepted Date: 5 July 2015

Please cite this article as: Karatay A, Miser MC, Cui X, Küçüköz B, Yılmaz H, Sevinç G, Akhüseyin E, Wu X, Hayvali M, Yaglioglu HG, Zhao J, Elmali A, The Effect of Heavy Atom to Two Photon Absorption Properties and Intersystem Crossing Mechanism in Aza-Boron-Dipyrromethene Compounds, *Dyes and Pigments* (2015), doi: 10.1016/j.dyepig.2015.07.002.

This is a PDF file of an unedited manuscript that has been accepted for publication. As a service to our customers we are providing this early version of the manuscript. The manuscript will undergo copyediting, typesetting, and review of the resulting proof before it is published in its final form. Please note that during the production process errors may be discovered which could affect the content, and all legal disclaimers that apply to the journal pertain.



# The Effect of Heavy Atom to Two Photon Absorption Properties and Intersystem Crossing Mechanism in Aza-Boron-Dipyrromethene Compounds

Ahmet Karatay,<sup>a</sup> M. Ceren Miser,<sup>b</sup> Xiaoneng Cui,<sup>c</sup> Betül Küçüköz,<sup>a</sup> Halil Yılmaz,<sup>b</sup> Gökhan Sevinç,<sup>b</sup> Elif Akhüseyin,<sup>a</sup> Xueyan Wu,<sup>c</sup> Mustafa Hayvali,<sup>\*b</sup> H. Gul Yaglioglu,<sup>\*a</sup> Jianzhang Zhao,<sup>c</sup> Ayhan Elmali<sup>a</sup>

<sup>a</sup> Department of Engineering Physics, Faculty of Engineering, Ankara University, 06100 Beşevler, Ankara, Turkey

<sup>b</sup> Department of Chemistry, Faculty of Science, Ankara University, 06100 Beşevler, Ankara, Turkey

<sup>c</sup> Dalian University of Technology, State Key Laboratory of Fine Chemicals, School of Chemical Engineering, E-208 West Campus, 2 Ling-Gong Road, Dalian 116024, P. R. China

**ABSTRACT**

New aza-boron-dipyrromethene compounds containing bromine atoms at various positions were designed and synthesized to enhance the triplet state population and two photon absorption properties for applications such as two-photon photodynamic therapy, triplet-triplet annihilation up-conversion. Steady state fluorescence and ultrafast pump probe spectroscopy techniques revealed that only 2, 6 positions of aza-boron-dipyrromethene core contribute to triplet state population significantly. Density function theory calculations showed that when bromine atoms introduced to 2, 6 position of aza-boron-dipyrromethene core, singlet and triplet energy levels get closer therefore probability of intersystem crossing increases. Z-scan experiments at 800 nm wavelengths revealed considerably large (610 GM) two photon absorption cross section value with respect to literature for compounds showing intersystem crossing mechanism. The efficient intersystem crossing and enhanced two-photon absorption properties make the investigated aza-boron-dipyrromethene compounds good candidates for two-photon photodynamic therapy application.

**KEYWORDS** Aza-boron-dipyrromethene, Heavy atom effect, Ultrafast pump probe spectroscopy, Intersystem crossing, Two photon absorption, Z-scan technique

\* Corresponding authors. Tel./Fax: +90 (312) 2232395 (M. H.), Tel./Fax:+90 (312) 2127343 (H. G. Y.).

E-mail addresses: yoglu@eng.ankara.edu.tr (H.G. Yaglioglu); hayvali@science.ankara.edu.tr

(M. Hayvali)

## 1. Introduction

There has been a great deal of interest on intersystem crossing (ISC) process of novel materials due to their related applications in photochemical and photophysical processes, such as photodynamic therapy (PDT) [1-5], photocatalytic organic reactions [6-11], triplet-triplet annihilation (TTA), upconversion (UC), and singlet oxygen generation [12,13]. ISC process is an efficient way to generate singlet oxygen especially for PDT application. The spin-orbit perturbation of electronic states plays an important role on the photophysical properties of organic molecules. Introducing heavy atoms to molecular systems increases ISC process and therefore, changes photophysical properties, which is known as heavy atom effect [14]. Enhanced spin-orbit perturbations can be achieved by introducing a heavy atom directly onto the absorbing core of the molecule (internal heavy atom effect) [15, 16] or by positioning heavy atoms to the peripheral positions (external heavy atom effect) [13, 17, 18]. Internal heavy atom effect is the most efficient way to enhance ISC process. Therefore, the effects of heavy atom on the photoinduced electron transfer mechanism to the triplet state have been extensively studied [1, 19].

On the other hand, organic molecules with large two photon absorption (TPA) properties have attracted increasing attention due to a wide range of potential applications including optical limiting [20,21], TPA imaging microscopy [22], three-dimensional microfabrication [23,24], optical data storage [25,26], TPA upconversion lasing [27], and especially for two-photon PDT [28]. Therefore, design and synthesis of molecules with large TPA cross-sections (TPCS) become a popular research field [29, 30]. Two-photon PDT application requires efficient ISC mechanism and high TPCS at near-IR region due to its low energy, deep penetration and negligible damage to the normal biological tissue. However, near-IR TPA photodynamic therapy is limited due to lack of TPA photosensitizer with high intersystem crossing rate and large TPCS.

There have been several studies about the application of aza-boron-dipyrromethene (aza-BODIPY) compounds to one photon PDT in the literature [1, 31]. Our previous research on aza-BODIPY compounds show that these compounds exhibit TPA properties [32, 33]. In this work, we designed and synthesized new aza-BODIPY compounds possessing both ISC and TPA properties for PDT applications.

In literature, heavy atom effect on photophysical properties of organic molecules and complexes of various types of molecules such as meso-tetraaryl porphyrins for selenium atoms [34, 35], poly halogenated *meso*-tetraaryl porphyrins and bacteriochlorins molecules [36, 37], BODIPY [38, 39], and aza-BODIPY [40-42] compounds were studied. Heavy atoms introduced to 2,6 position of aza-BODIPY core are known to enhance the probability of ISC due to internal heavy atom effect (i.e. spin orbit coupling) [14-16]. This effect was investigated by monitoring fluorescence, phosphorescence and singlet oxygen quantum yields [1, 39, 43, 44]. It is known that number of heavy atoms introduced to BODIPY core other than 2,6 positions do not affect ISC [43]. However, it is not clear, how do heavy atoms on the peripheral positions effect ISC in the literature for aza-BODIPY compound. Therefore, our designed and synthesized new aza-BODIPY compounds contain Br atoms at various positions. Previous works investigating the heavy atom effects on the triplet population used indirect methods such as singlet oxygen quantum yields. We investigated their triplet level populations by using ultrafast pump probe spectroscopy technique. This technique is a very sensitive tool to investigate directly the transition of triplet to levels with fs time resolution. In order to clarify our experimental results and reveal the mechanism causing ISC, we performed density functional theory (DFT) calculations for our investigated compounds.

## 2. Result And Discussion

### 2.1 Absorption and Fluorescence Measurement

UV-Vis absorption and emission spectra of **4a-d** and **5a-d** are shown in Fig. 1 and Fig. 2, respectively. Absorption spectrum of **4a** compound reveals  $S_0 \rightarrow S_1$  transition with maximum absorbance wavelength at 650 nm in Fig. 1. However,  $S_0 \rightarrow S_1$  transition of Br containing compounds is between 645 nm and 667 nm. This spectral shift depends on the position of Br atoms on aza-BODIPY core. Bathochromic shifts were observed when Br atoms on the para positions of the phenyl ring on the any of 1,7 and 3,5 positions (**4b-d**, **5b-d**) as seen in Table 1. On the contrary, directly introducing of Br atoms to 2,6 position of aza-BODIPY core leads to hypsochromic shifts (**5a-d**). Interestingly, the amounts of spectral shift per binding position, whether it is bathochromic or hypsochromic are the same. Therefore, these bathochromic or hypsochromic spectral shifts cancel each other for **4a**, **5b** and **5c** compounds and the absorption bands of these compounds are localized around 650 nm. In addition, FWHM values for studied compounds increases with increasing the number of the heavy atoms (Table 1).

On the other hand, another absorption band is observed at 320 nm which corresponds to  $S_0 \rightarrow S_2$  transition of aza-BODIPY compounds without containing Br atoms at 2,6 position. Upon introducing Br atoms at 2,6 position of aza-BODIPY, significant hypsochromic shift (about 20 nm) was observed for  $S_0 \rightarrow S_2$  transition.

It is known that aza-BODIPY compounds have high fluorescence quantum yields [45]. A single fluorescence signals were observed for **4a-d** compounds as seen in Fig. 2. The fluorescence intensity increases with increasing number of binding *p*-Br phenyl groups to 1,7,3,5 positions of aza BODIPY core. Therefore, **4d** compound containing *p*-Br phenyl at 1,7,3,5 positions shows the highest fluorescence intensity while **4a** compound has the lowest fluorescence intensity among these compounds. On the other hand, it is well known that the introducing Br atoms to 2,6 positions makes singlet-triplet transition easier [41]. Therefore, in

our studied compounds, fluorescence signal drastically decrease for **5a-d** compounds containing Br atoms at 2,6 position of aza-BODIPY core due to the ISC process. This decreased fluorescence signal may indicate that our low fluorescent compounds may have efficient ISC due to heavy atom effect. In order to obtain more information about the effect of heavy atom on aza-BODIPY compounds by changing position and number of heavy atoms, we performed ultrafast pump probe spectroscopy experiments.

## 2.2 Ultrafast Pump Probe Spectroscopy

Ultrafast pump probe spectroscopy experiments were used to investigate the effect of heavy atom and its position on ISC mechanism and decay processes of excited states of the aza-BODIPY compounds. Femtosecond transient absorption spectra with 640 nm excitation wavelength for **4a** and **5a** compounds in THF are given in Fig. **3a** and **3b**, respectively. The results of experiments show different characteristics depending on the position and the number of heavy atom. Transient absorption spectra of **4a** have a great bleach signal at 650 nm and excited state absorption signal below 575 nm and above 750 nm as shown in Fig. **3a**. **4b-d** compounds also show similar transient absorption spectra characteristics. However, linear and transient absorption spectra of compound **5a** have different characteristics. For instance, vibration states appearing around 520 nm in linear absorption spectra get higher absorption peak when Br atoms bond to 2,6 position of aza-BODIPY core. That causes an extra bleach signal to appear around 520 nm in transient absorption spectra as seen in Fig. **3b**. In addition to that, an excited state absorption (ESA) signal appears in transient absorption spectra at about 120 ps time delay and around 695 nm wavelength, which can be attributed to  $T_1$ - $T_n$  transition (Fig. **3b**, Fig. **4**). Similar spectral properties were also observed for other Br compounds containing Br atoms at 2,6 position of aza-BODIPY core (**5a-d**). These experimental data were given in supporting information.

Another evidence of ISC mechanism is clearly observed from the decay curves seen in Fig. 5. The lifetime of the bleach signals show great differences whether including Br atoms at 2,6 position of aza-BODIPY core or not. There is a long time component (with decay time about  $\mu\text{s}$  range) for **5a-d** compounds. This component can be attributed to lifetime of the triplet states of the aza-BODIPY. These experimental results indicate that only Br atoms at 2,6 positions enhance the ISC mechanism due to the internal heavy atom effect [7]. Enhanced ISC mechanism also causes fluorescence signal reducing drastically as observed in the fluorescence measurements in Fig. 2.

Moreover, different decay curves were recorded for **4a** and **4d** compounds as seen in Fig. 6. The excited state lifetime of the **4d** compound is longer than that of **4a** compound. It may be due to heavy atom effect since it contains more Br atoms.

In an attempt to clarify the reason why compounds **5a-d** showing stronger ISC than **4a-d** compounds we performed DFT calculations for these compounds.

### 2.3 DFT Calculations on the Photophysical Properties of the Complexes

The ground state geometries of the compounds were optimized with the DFT theory. The aza-BODIPY core takes a planar geometry. Interestingly, the four phenyl rings take a nearly co-planar geometry orientation toward the aza-BODIPY core, even with a perpendicular initial geometry for the DFT calculation. This result indicates that the coplanar geometry is at least a local energy minimum. For example, the dihedral angle between the phenyl ring (close to the  $\text{BF}_2$  complexation site) and the aza-BODIPY core is ca.  $31^\circ$ . For the phenyl rings at the opposite position of the  $\text{BF}_2$  complexation, the dihedral angle is smaller ( $24^\circ$ ), probably due to the smaller steric hindrance. Similar results were found for all the compounds **4b-4c** (see Supporting Information). The  $T_1$  triplet state energy of **4a** was calculated as 1378 nm (0.90 eV), which is close to a previously reported value (0.87 eV) [46].

The excited state of compound **4a** was calculated. The UV-Vis absorption maximum is predicted at 605 nm, which is close, the experimental result of 650 nm. The deviation is known for the calculation of BODIPY compounds with the DFT theory (Fig. 7). The frontier molecular orbitals are delocalized on the aza-BODIPY core and the appended phenyl rings.

Similarly, the geometry of the ground state of the 2,6-dibromo aza-BODIPYs (**5a-5d**) was also optimized. Interestingly, we found that the dihedral angles between the phenyl rings and the aza-BODIPY core are increased, that is, the moieties in the molecules are less coplanar. For example, the dihedral angle between the phenyl rings (close to the BF<sub>2</sub>complexation site) and the aza-BODIPY core is ca. 51°. For the phenyl rings on the opposite to the BF<sub>2</sub>complexation site, dihedral angle of ca. 41° was found. These angles are much larger than that observed for the unbrominated compounds **4a-4d**. These changes are probably due to the steric hindrance of the bromine atoms at the 2,6 position of the aza-BODIPY core.

The excited states of compound **5a** were also studied with the DFT calculations (Table 2) (Fig. 8). Interestingly, shorter wavelength for UV-vis absorption band was found for **5a** as compared with that of **4a**. For example, the first absorption band was predicted as 581 nm for **5a**, as compared with that of 605 nm for **4a** (Table 3). This blue-shifted absorption of **5a** as compared with **4a** may be due to the poor planar geometry of the molecule, as predicted by the DFT calculations on the ground state geometry.

The T<sub>1</sub> state energy level of **5a** was calculated as 0.98 eV (1267 nm). Thus **5a** can be used as triplet photosensitizer for photosensitizing of singlet oxygen (<sup>1</sup>O<sub>2</sub>). This theoretical prediction is in agreement with the experimental results [1, 47].

The spin density surfaces of the compounds were studied with the optimized triplet state geometry, so that the distribution of the triplet states of the compounds were unveiled (Fig. 9) [48]. For compound **4a**, the triplet state is delocalized over the entire molecule.

Similar results were found for **4b-4d** (see Supporting Information). For **5a**, similar results were observed. Note the bromine atoms contribute to the spin density surface, thus intersystem crossing is expected for compound **5a**.

DFT calculations revealed that singlet energy levels decrease and get closer to triplet energy levels due to conformation transformation upon excitation for samples **5a-d** (Fig. S26). Decreasing singlet energy levels increase probability of ISC to triplet levels. This can be attributed to spin-orbit coupling (heavy atom effect). Fluorescence quenching (Fig. 2) and pump-probe experimental results (Fig. 3, 4) for these compounds support DFT calculations. On the other hand heavy atoms that are not located at the core of aza-BODIPY (compounds **4a-d**) do not affect conformation transformation and therefore ISC probability is lower for these molecules (Fig. 3, 4).

#### 2.4 Two Photon Absorption Properties

It is known that TPA properties are improved upon increasing charge transfer for BODIPY and aza-BODIPY compounds [49-51]. Therefore, in an attempt to find out whether charge transfer to triplet state affects TPA properties, we investigated number and position effects of Br atoms on TPA properties by OA Z-scan technique [49]. TPA coefficient ( $\beta$ ) and TPCS ( $\sigma_2$ ) were calculated from the following equations [51].

Nonlinear transmittance  $T$  is given in terms of laser intensity  $I_0$ ,

$$T(I_0) = \frac{1}{1 + I_0 \beta l} \quad (1)$$

where,  $l$  is optical path length.  $\beta$  value is obtained from the curve fitting the OA Z-scan data to equation 1. TPCS value  $\sigma_2$  ( $1 \text{ GM} = 10^{-50} \text{ cm}^4 \text{ s photon}^{-1}$ ) is obtained by using  $\beta$  value in the following equation,

$$\sigma_2 = \frac{h\nu\beta}{N_A d_0 \times 10^{-3}} \quad (2)$$

where,  $N_A$  is the Avogadro number and  $d_0$  is molar concentration of the solution.

OA Z-scan experimental results of **5a-d** compounds as well as theoretical fits at **80 GW/cm<sup>2</sup>** peak intensities are shown in Fig. **10**. Calculated TPCS values are written in Table 1. TPA properties depend on both position and the number of Br atoms introduced to the phenyl rings at 1,3,5,7 positions. As seen from these results, when Br atoms are bound to 1,7 positions ( $\sigma_{5c}=444$  GM) TPCS value is greater than that of bound to 3,5 positions ( $\sigma_{5b}= 218$  GM). This result could be explained by considering our DFT calculation given in the previous section. According to DFT calculations, dihedral angle for 1,7 positions are smaller than that of 3,5 positions. It is known that greater dihedral angle causes smaller the charge transfer due to the non-planarity of the compound [52]. This explains why 1,7 position (compound **5c**) is more efficient for charge transfer than 3,5 positions (compound **5b**) for the investigated compounds.

Among **5a-d** compounds, **5d** has the highest TPCS value (610 GM). In the literature, there are only a few studies about TPA properties of aza-BODIPY compounds [41, 50, 32]. The highest TPCS value was measured about 30 GM at 800 nm wavelength [41]. Our TPCS value (610 GM) is about twenty times greater than this value.

### 3. Conclusion

We synthesized and studied linear and nonlinear optical properties of aza-BODIPY compounds containing heavy atom with different numbers and positions. The effect of heavy atom on intersystem crossing mechanism of newly synthesized Br containing aza-BODIPY compounds were investigated using fluorescence and ultrafast pump probe spectroscopy experiments as well as density functional theory calculations. The fluorescence intensity

drastically decreased when compounds include heavy atoms at 2,6 position of the aza-BODIPY core as observed in the literature. Ultrafast pump probe experimental results explained observed fluorescence quenching by showing triplet state population when Br atoms are introduced to the 2,6 positions of aza-BODIPY core. Further, density functional theory calculations supported these findings by revealing that singlet and triplet levels get closer to each other when Br atoms are at 2,6 position of aza-BODIPY core. Our experimental and theoretical investigations showed that introducing Br atoms on peripheral positions of aza-BODIPY compounds does not affect the triplet state populations. Open aperture Z-scan experiments at 800 nm wavelengths revealed considerably large (610 GM) two photon absorption cross section values for investigated compounds showing intersystem crossing mechanism. This value at 800 nm wavelengths is much greater than that of aza-BODIPY compounds in the literature at this wavelength, which is important for photodynamic therapy application. Experimental findings also revealed that binding of phenyl rings affect two photon absorption properties considerably. Our studied compounds with high intersystem crossing mechanism and enhanced two photon absorption properties at 800 nm wavelengths may be good candidates for two-photon photodynamic therapy applications. On the other hand, observed weak fluorescence signal and high two-photon absorption cross section value may be useful for fluorescence and two-photon fluorescence imaging applications. Therefore, we believe this work gives valuable contribution to design new compounds for two photon absorption applications.

## **4. Experimental Section**

### 4.1 Syntheses of Studied Compounds

#### *4.1.1 General*

All solvents and reagents were purchased from Sigma-Aldrich Chemical Company and used as received without further purification. Reactions were monitored by thin layer chromatography using fluorescent coated aluminum sheets (Merck 60 PF-254). Compounds **1a-d**, **2a-d**, **3a-d**, **4a-c**, **5a** were prepared according to the literature [1,53,54].

#### 4.1.2 Characterization

Melting points were determined on a Gallenkamp melting point platform. Flash column chromatography was carried out using silica columns on Combi Flash Rf 200 (Teledyne-Isco, Lincoln, NE) instruments unless otherwise mentioned. The IR spectra were recorded using Shimadzu Infinity model FTIR spectrometer equipped three reflections ATR attachment. Mass spectral analyses were performed with a Waters 2695 Alliance MicromassZQ LC/MSspectrometer.  $^1\text{H}$  NMR spectra were recorded with a VARIAN Mercury 400 MHz spectrometer.  $^1\text{H}$  NMR chemical shifts ( $\delta$ ) are given in ppm downfield from  $\text{Me}_4\text{Si}$ , determined by chloroform ( $\delta = 7.26$  ppm).  $^{13}\text{C}$  NMR spectra were recorded with a VARIAN Mercury 100 MHz spectrometer.  $^{13}\text{C}$  NMR chemical shifts ( $\delta$ ) are reported in ppm with the internal  $\text{CDCl}_3$  at  $\delta$  77.0 ppm as standard.

#### 4.1.2 Syntheses of Compounds

**Synthesis Compound 4d:** A solution of compound **3d** (0.23 g, 0.30 mmol) in dry  $\text{CH}_2\text{Cl}_2$  (100 mL) was treated with diisopropylethylamine (0.52 mL, 3.00 mmol) and the mixture was stirred for 10 min at room temperature. Then, boron trifluoridediethyletherate (0.55 mL, 4.50 mmol) was added and the reaction mixture was stirred at room temperature for 24 h. The mixture was washed with water, and the organic layer dried over sodium sulfate. Removal of solvent gave a residue, which was purified by flash chromatography on silica eluting with hex/EtOAc (2:1) resulting the product as a dark blue solid (0.20 g, 83%), mp 270-273 °C.  $^1\text{H}$ NMR (400 MHz,  $\text{CDCl}_3$ )  $\delta$  7.89 (d,  $J = 8.4$  Hz, 6H), 7.64-7.60 (m, 10H), 7.00

(s, 2H),  $^{13}\text{C}$  NMR (100 MHz,  $\text{CDCl}_3$ )  $\delta$  132.3, 132.1, 131.8, 131.5, 131.4, 129.4, 128.9, 128.0, 126.5, 125.1; IR ( $\text{cm}^{-1}$ ): 1581.6, 1292.3, 1232.5; Anal. Calcd. for  $\text{C}_{32}\text{H}_{18}\text{BBr}_4\text{F}_2\text{N}_3$ : C, 47.28; H, 2.23; N, 5.17. Found: C, 47.06; H, 2.14; N, 5.23; ES/MS calculated for 812.9, found 813.7.

**Synthesis Compound 5b:** A solution of compound **4b** (0.21 g, 0.32 mmol) in dry  $\text{CH}_2\text{Cl}_2$  (60 mL) was added to N-bromosuccinimide (NBS) (0.12g, 0.68 mmol), and the mixture was stirred at room temperature for 24 h. After the reaction was completed, the solvent was evaporated under reduced pressure. The residue was washed with water and dried over sodium sulfate. The residual was purified by flash chromatography on silica eluting with hex/EtOAc (2:1) which gave the product as a dark blue solid (0.20 g, 76%), mp 283 °C.  $^1\text{H}$ NMR (400 MHz,  $\text{CDCl}_3$ )  $\delta$  7.87-7.85 (m, 4H), 7.62 (s, 8H), 7.47-7.45 (m, 6H),  $^{13}\text{C}$  NMR (100 MHz,  $\text{CDCl}_3$ )  $\delta$  157.3, 144.4, 143.3, 131.9, 131.5, 130.7, 130.3, 130.1, 129.9, 128.7, 128.1, 126.0; IR ( $\text{cm}^{-1}$ ): 1587.4, 1313.5, 1296.2; Anal. Calcd. for  $\text{C}_{32}\text{H}_{18}\text{BBr}_4\text{F}_2\text{N}_3$ : C, 47.28; H, 2.23; N, 5.17. Found: C, 46.83; H, 2.32; N, 5.09; ES/MS calculated for 812.9 found 813.0.

**Synthesis Compound 5c:** A solution of compound **4c** (0.20 g, 0.31 mmol) in dry  $\text{CH}_2\text{Cl}_2$  (60 mL) was added to N-bromosuccinimide (NBS) (0.12 g, 0.68 mmol), and the mixture was stirred at room temperature for 24 h. After the reaction was completed, the solvent was evaporated under reduced pressure. The residue was washed with water, and dried over sodium sulfate. The residual was purified by flash chromatography on silica eluting with hex/EtOAc (2:1) which gave the product as a dark blue solid (0.14 g, 56%), mp 245 °C.  $^1\text{H}$ NMR (400 MHz,  $\text{CDCl}_3$ )  $\delta$  7.74 (d,  $J = 8.4$  Hz, 4H), 7.71 (d,  $J = 8.0$  Hz, 4H), 7.60 (d,  $J = 8.4$  Hz, 4H), 7.50-7.47(m, 6H),  $^{13}\text{C}$  NMR (100 MHz,  $\text{CDCl}_3$ )  $\delta$  159.0, 144.3, 141.9, 146.0, 132.3, 131.7, 131.3, 130.5, 129.6, 129.3, 128.3, 124.9, 110.8; IR ( $\text{cm}^{-1}$ ): 1587.4, 1274.9, 1222.9; Anal. Calcd. for  $\text{C}_{32}\text{H}_{18}\text{BBr}_4\text{F}_2\text{N}_3$ : C, 47.28; H, 2.23; N, 5.17. Found: C, 46.92; H, 2.28; N, 5.11; ES/MS calculated for 812.9 found 813.1.

**Synthesis Compound 5d:** A solution of compound **4d** (0.10 g, 0.13 mmol) in dry  $\text{CH}_2\text{Cl}_2$  (20 mL) was added to N-bromosuccinimide (NBS) (0.05g, 0.28 mmol), and the mixture was stirred at room temperature for 24 h. After the reaction was completed, the solvent was evaporated under reduced pressure. The residue was washed with water, and dried over sodium sulfate. The residual was purified by flash chromatography on silica eluting with hex/EtOAc (2:1) which gave the product as a dark blue solid (0.05 g, 38%), mp>300 °C.  $^1\text{H}$ NMR (400 MHz,  $\text{CDCl}_3$ )  $\delta$  7.72 (d,  $J$  = 8.8 Hz, 4H), 7.64-7.58 (m, 12H),  $^{13}\text{C}$  NMR (100 MHz,  $\text{CDCl}_3$ )  $\delta$  144.3, 142.1, 132.0, 131.8, 131.5, 129.2, 127.8, 126.2, 124.9; IR ( $\text{cm}^{-1}$ ): 1587.4, 1311.6, 1296.2; Anal. Calcd. for  $\text{C}_{32}\text{H}_{16}\text{BBr}_6\text{F}_2\text{N}_3$ : C, 39.59; H, 1.66; N, 4.33. Found: C, 39.83; H, 1.41; N, 4.49. ES/MS calculated for 970.7 found 971.8.

#### 4.2 Optical Measurements

The UV-Vis absorption spectra of aza-BODIPY derivatives were recorded using a scanning spectrophotometer (Shimadzu UV- 1800). The fluorescence measurements were obtained with a Perkin Elmer model LS 55 fluorescence spectrometer. All fluorescence spectra were obtained at  $1 \times 10^{-5}$  M concentration in THF solution by using 10 mm quartz cell.

Ultrafast pump probe spectroscopy measurements were performed using Ti:Sapphire laser amplifier, optical parametric amplifier system with 45 fs pulse duration and 1 kHz repetition rate (Spectra Physics, Spitfire Pro XP, TOPAS). In order to investigate effect of the heavy atom on ISC mechanisms and excited state lifetime, commercial pump probe experimental setup (Spectra Physics, Helios) with white light continuum probe was used. The pump wavelength was chosen for ultrafast pump probe spectroscopy experiments according to maximum absorption wavelength of the investigated samples. Pulse duration was measured as 120 fs inside the pump probe setup.

Nonlinear optical absorption properties of aza-BODIPY derivatives were investigated by using open aperture (OA) Z-scan technique [55]. Laser source is mode-locked Ti:Sapphire

laser amplifier system with 800 nm wavelength, 1 ps pulse duration and 1 kHz repetition rate (Spectra Physics, Spitfire Pro XP, TOPAS). Laser beam was focused on solution in 1 mm thick cell by a lens with 20 cm focal length. Concentrations of the solutions for two photon absorption measurements were 0.005 M. **4a-d** compounds have linear absorption at 800 nm wavelength for 0.005 M. Therefore, OA Z-scan experiments were not performed for these compounds. TPA properties of compounds 5a-d were investigated and compared with each other.

#### 4.3 DFT Calculation

The DFT calculations were used for optimization of both singlet states and triplet states. The UV-Vis absorption and the energy level of the T1 state were calculated with the time dependent DFT (TDDFT), based on the optimized singlet ground state geometries ( $S_0$  state). The spin density surface of the complexes was calculated based on the optimized triplet state. All the calculations were performed at the B3LYP/GENECP/LANL2DZ level with Gaussian 09W [56].

#### REFERENCES

- [1] Gorman A, Killoran J, O'Shea C, Kenna T, Gallagher WM, O'Shea DF. In Vitro Demonstration of the Heavy-Atom Effect for Photodynamic Therapy. *J. Am. Chem. Soc* 2004; 126:10619–10631.
- [2] McDonnell SO, Hall MJ, Allen LT, Byrne A, Gallagher WM, O'Shea DF. Supramolecular Photonic Therapeutic Agents. *J. Am. Chem. Soc* 2005; 127:16360–16361.
- [3] Kamkaew A, Lim SH, Lee HB, Kiew LV, Chung LY, Burgess K. BODIPY Dyes in Photodynamic Therapy. *Chem. Soc. Rev* 2013; 42:77–88.
- [4] Cakmak Y, Kolemen S, Duman S, Dede Y, Dolen Y, Kilic B, Kostereli Z, Yildirim LT, Dogan AL, Guc D, Akkaya EU. Designing Excited States: Theory-Guided Access to Efficient Photosensitizers for Photodynamic Action. *Angew. Chem. Int. Ed* 2011; 123:12143–12147.

- [5] O'Connor AE, Gallagher WM, Byrne AT. Porphyrin and Nonporphyrin Photosensitizers in Oncology: Preclinical and Clinical Advances in Photodynamic Therapy. *Photochem. Photobiol* 2009; 85:1053–1074.
- [6] Xuan J, Xiao WJ. Visible-Light Photoredox Catalysis. *Angew. Chem. Int. Ed* 2012; 51:6828–6838.
- [7] Shi L, Xia W. Photoredox Functionalization of C–H Bonds Adjacent to a Nitrogen Atom. *Chem. Soc. Rev* 2012; 41:7687–7697.
- [8] Ravelli D, Fagnoni M, Albini A. Photoorganocatalysis. What for?. *Chem. Soc. Rev* 2013; 42:97–113.
- [9] Maity S, Zhu M, Shinabery RS, Zheng N. Intermolecular [3+2] Cycloaddition of Cyclopropylamines with Olefins by Visible-Light Photocatalysis. *Angew. Chem. Int. Ed* 2012; 51:222–226.
- [10] Neumann M, Földner S, König B, Zeitler K. Metal-Free, Cooperative Asymmetric Organophotoredox Catalysis with Visible Light. *Angew. Chem. Int. Ed* 2011; 50:951–954.
- [11] Zou YQ, Lu LQ, Fu L, Chang NJ, Rong J, Chen JR, Xiao WJ. Visible-Light-Induced Oxidation/[3+2] Cycloaddition/Oxidative Aromatization Sequence: A Photocatalytic Strategy to Construct Pyrrolo[2,1-a]isoquinolines. *Angew. Chem. Int. Ed* 2011; 50:7171–7175.
- [12] Schweitzer C, Schmidt R. Physical Mechanisms of Generation and Deactivation of Singlet Oxygen. *Chem. Rev* 2003; 103:1685–1757.
- [13] Koziar JC, Cowan DO. Photochemical Heavy-Atom Effects. *Acc. Chem. Res* 1978; 11:334–341.
- [14] Sauerwein B, Schuster GB. External Iodine Atoms Influence Over the Intersystem Crossing Rate of Cyanine Iodide Ion Pair in Benzene Solution. *J. Phys. Chem* 1991; 95:1903–1906.
- [15] Yuster P, Weissman SI. Effects of Perturbations on Phosphorescence: Luminescence of Metal Organic Complexes. *J. Chem. Phys* 1949; 17:1182–1188.
- [16] McClure DS. Triplet-Singlet Transitions in Organic Molecules. Lifetime Measurements of the Triplet State. *J. Chem. Phys* 1949; 17:905–913.
- [17] McGlynn SP, Reynolds MJ, Daigre GW, Christodouleas NDJ. The External Heavy-Atom Spin-Orbital Coupling Effect. III. Phosphorescence Spectra and Lifetimes of Externally Perturbed Naphthalenes<sup>1,2</sup>. *J. Phys. Chem* 1962; 66:2499–2505.
- [18] Kasha MJ. Collisional Perturbation of Spin-Orbital Coupling and the Mechanism of Fluorescence Quenching. A Visual Demonstration of the Perturbation. *J. Chem. Phys* 1952; 20:71–74.
- [19] (a) Zhang X, Xiao Y, Qi J, Qu J, Kim B, Yue X, Belfield KD. Long-Wavelength, Photostable, Two-Photon Excitable BODIPY Fluorophores Readily Modifiable for Molecular Probes. *J. Org. Chem* 2013; 78: 9153–9160;

- (b) Solovyov KN, Borisevich EA. Intramolecular heavy-atom effect in the photophysics of organic molecules. *Physics – Uspekhi* 2005; 48:231 – 253; (c) Zhao J, Wu W, Sun J, Guo S. Triplet photosensitizers: from molecular design to applications. *Chem. Soc. Rev* 2013; 42:5323-5351.
- [20] He GS, Xu GC, Prasad PN, Reinhardt BA, Bhatt JC, Dillard AG. Two-photon absorption and optical-limiting properties of novel organic compounds. *Opt. Lett* 1995; 20:435-437.
- [21] Ehrlich JE, Wu XL, Lee IYS, Hu ZY, Röckel H, Marder SR, Perry JW. Two-photon absorption and broadband optical limiting with bis-donor stilbenes. *Opt. Lett* 1997; 22:1843-1845.
- [22] Kasischke KA, Wishwasrao HD, Fisher PJ, Zipfel WR., Webb WW. Neutral activity triggers neuronal oxidative metabolism followed by astrocytic glycolysis. *Science* 2004; 305: 99-103.
- [23] Kawata S, Sun HB, Tanaka T, Takada K. Finer features for functional microdevices. *Nature* 2001; 412:697-698.
- [24] Zhou W, Kuebler SM, Braun KL, Yu T, Cammack JK, Ober CK, Perry JW, Marder SR. An efficient two-photon-generated photoacid applied to positive-tone 3D microfabrication. *Science* 2002; 296:1106-1109.
- [25] Cumpston BH, Ananthavel SP, Barlow S, Dyer DL, Ehrlich JE, Erskine LL, Heikal AA, Kuebler SM, Lee IYS, McCord-Maughon D, Qin JG, Röckel H, Rumi M, Wu XL, Marder SR, Perry JW. Two-photon polymerization initiator for three-dimensional optical data storage and microfabrication. *Nature* 1999; 398: 51-54.
- [26] Parthenopoulos DA, Rentzepis PM. Three-dimensional optical storage memory. *Science* 1989; 245: 843-845.
- [27] Bhawalkar JD, He GS, Park CK, Zhao CF, Ruland G, Prasad PN. Efficient, two-photon pumped green upconverted cavity lasing in a new dye. *Opt. Commun* 1996; 124: 33-37.
- [28] Bhawalkar JD, Kumar ND, Zhao CF, Prasad PN. Two-photon photodynamic therapy. *J. Clin. Laser Med. Surg* 1997; 15:201-204.
- [29] Albota M, Beljonne D, Bredas JL, Ehrlich JE, Fu JY, Heikal AA, Hess SE, Kogej T, Levin MD, Marder SR, McCord-Maughon D, Perry JW, Rockel H, Rumi M, Subramaniam G, Webb WW, Wu XL, Xu C. Design of organic molecules with large two-photon absorption cross sections. *Science* 1998; 281:1653–1656.
- [30] Kogej T, Beljonne D, Meyers F, Perry JW, Marder SR, Bredas JL. Mechanism for enhancement of two-photon absorption in donor–acceptor conjugated chromophores. *Chem. Phys. Lett* 1998; 298:1–6.

- [31] Killoran J, Allen L, Gallagher JF, Gallagher WM, O'Shea DF. Synthesis of BF<sub>2</sub> chelates of tetraarylazadipyrromethenes and evidence for their photodynamic therapeutic behavior. *Chem. Commun* 2002; 17:1862-1863.
- [32] Küçüköz B, Hayvalı M, Yılmaz H, Uğuz B, Kürüm U, Yaglioglu HG, Elmali A. Synthesis, optical properties and ultrafast dynamics of aza-boron-dipyrromethene compounds containing methoxy and hydroxy groups and two-photon absorption cross-section. *J. Photochem. Photobio.A: Chem* 2012; 247:24-29.
- [33] Tekin S, Küçüköz B, Yılmaz H, Sevinç G, Hayvalı M, Yaglioglu HG, Elmali A. Enhancement of two photon absorption properties by charge transfer in newly synthesized aza-boron-dipyrromethene compounds containing triphenylamine, 4-ethynyl-N,N-dimethylaniline and methoxy moieties. *J. Photochem. Photobio.A: Chem* 2013; 256:23– 28.
- [34] You Y, Gibson SL, Hilf R, Davies SR, Oseroff AR, Roy I, Ohulchanskyy TY, Bergey EJ, Detty MR. Water Soluble, Core-Modified Porphyrins. 3. Synthesis, Photophysical Properties, and in Vitro Studies of Photosensitization, Uptake, and Localization with Carboxylic Acid-Substituted Derivatives. *J. Med. Chem* 2003; 46:3734–3747.
- [35] Hilmey DG, Abe M, Nelen MI, Stilts CE, Baker GA, Baker SN, Bright FV, Davies SR, Gollnick SO, Oseroff AR, Gibson SL, Hilf R, Detty MR. Water-Soluble, Core-Modified Porphyrins as Novel, Longer-Wavelength-Absorbing Sensitizers for Photodynamic Therapy. II. Effects of Core Heteroatoms and Meso-Substituents on Biological Activity. *J. Med. Chem* 2002; 45:449–461.
- [36] Pineiro M, Rocha Gonsalves AMd'A, Pereira MM, Formosinho SJ, Arnaut LG. New Halogenated Phenylbacteriochlorins and Their Efficiency in Singlet-Oxygen Sensitization. *J. Phy. Chem. A* 2002; 106:3787–3795.
- [37] Azenha EG, Serra AC, Pineiro M, Pereira MM, de Melo JS, Arnaut LG, Formosinho SJ, Rocha Gonsalves AMd'A. Heavy-Atom Effects on Metalloporphyrins and Polyhalogenated Porphyrins. *Chem. Phy* 2002; 280:177–190.
- [38] Jiao L, Pang W, Zhou J, Wei Y, Mu X, Bai G, Hao E. Regioselective Stepwise Bromination of Boron Dipyrromethene (BODIPY) Dyes. *J. Org. Chem* 2011; 76:9988–9996.
- [39] Awuah SG, Polreis J, Biradar V, You Y. Singlet Oxygen Generation by Novel NIR BODIPY Dyes. *Org. Lett* 2011; 13:3884-3887.
- [40] Guennic BL, Maurya O, Jacquemin D. aza-boron-dipyrromethene Dyes: TD-DFT Benchmarks, Spectral Analysis and Design of Original Near-IR Structures. *Phys. Chem. Chem. Phys* 2012; 14:157–164.

- [41] Batat P, Cantuel M, Jonusauskas G, Scarpantonio L, Palma A, O'Shea DF, McClenaghan ND. BF2-azadipyrrromethenes: Probing the Excited-State Dynamics of a NIR Fluorophore and Photodynamic Therapy Agent. *J. Phys. Chem. A* 2011; 115:14034–14039.
- [42] Adarsh N, Avirah RR, Ramaiah D. Tuning Photosensitized Singlet Oxygen Generation Efficiency of Novel aza-BODIPY Dyes. *Org. Lett* 2010; 12:5720-5723.
- [43] Ortiz MJ, Agarrabeitia AR, Duran-Sampedro G, Banuelos Prieto J, Lopez TA, Massad WA, Montejano HA, Garcia NA, Lopez AI. Synthesis and functionalization of new polyhalogenated BODIPY dyes. Study of their photophysical properties and singlet oxygen generation. *Tetrahedron* 2012; 68:1153–1162.
- [44] Yogo T, Urano Y, Ishitsuka Y, Maniwa F, Nagano T. Highly Efficient and Photostable Photosensitizer Based on BODIPY Chromophore. *J. Am. Chem. Soc* 2005; 127:12162–12163.
- [45] Loudet A, Burgess K. BODIPY Dyes and Their Derivatives: Syntheses and Spectroscopic Properties. *Chem. Rev* 2007; 107:4891–4932.
- [46] Quartarolo AD, Russo N, Sicilia E. Structures and Electronic Absorption Spectra of a Recently Synthesised Class of Photodynamic Therapy Agents. *Chem. Eur. J* 2006; 12:6797 – 6803.
- [47] Adarsh N, Shanmugasundaram M, Avirah RR, Ramaiah D. aza-BODIPY Derivatives: Enhanced Quantum Yields of Triplet Excited States and the Generation of Singlet Oxygen and their Role as Facile Sustainable Photooxygenation Catalysts. *Chem. Eur. J* 2012; 18:12655 – 12662.
- [48] (a) Hanson K, Tamayo A, Diev VV, Whited MT, Djurovich PI, Thompson ME. Efficient Dipyrrin-Centered Phosphorescence at Room Temperature from Bis-Cyclometalated Iridium(III) Dipyrrinato Complexes. *Inorg. Chem* 2010; 49:6077–6084; (b) Wu W, Zhao J, Sun J, Guo S. Light- Harvesting Fullerene Dyads as Organic Triplet Photosensitizers for Triplet–Triplet Annihilation Upconversions. *J. Org. Chem* 2012; 77:5305–5312.
- [49] Wang Y, Zhang D, Zhou H, Ding, JC, Xiao Y, Qian S. Nonlinear optical properties and ultrafast dynamics of three novel boradiazaindacene derivatives. *J. Appl. Phys* 2010; 108:033520.
- [50] Bouit PA, Kamada K, Feneyrou P, Berginc G, Toupet L, Maury O, Andraud C. Two-photon absorption-related properties of functionalized BODIPY dyes in the infrared range up to telecommunication wavelengths. *Adv. Mater* 2009; 21:1151.
- [51] Zheng Q, He GS, Prasad PN. A novel near IR two-photon absorbing chromophore: optical limiting and stabilization performances at an optical communication wavelength. *Chem. Phys. Lett* 2009; 475: 250-255.

- [52] Knyukshto VN, Sagun EI, Shul'ga AM, Bachilo SM, Starukhin DA, Zen'kevich ÉI. Manifestation of Nonplanarity Effects and Charge-Transfer Interactions in Spectral and Kinetic Properties of Triplet States of Sterically Strained Octaethylporphyrins. *Optics And Spectroscopy* 2001; 90:67-77.
- [53] Bellier Q, Pegaz S, Aronica C, Le Guennic B, Andraud C, Maury O. Near-Infrared Nitrofluorene Substitued aza-Boron-dipyrromethenes Dyes. *Org. Lett* 2011; 13:22-25.
- [54] Gao L, Deligonul N, Gray GT. Gold (I) Complexes of Brominated azadipyrromethene Ligands. *Inorg. Chem* 2012; 51:7682–7688.
- [55] Sheik- Bahae M, Said AA, Wei TH, Hagan DJ, Stryland WV. Sensitive measurement of optical nonlinearities using a single beam. *IEEE Journal of Quantum Electronics* 1990; 26:760-769.
- [56] Frisch MJ, Trucks GW, Schlegel HB, Scuseria GE, Robb MA, Cheeseman JR, Scalmani G, Barone V, Mennucci B, Petersson GA, Nakatsuji H, Caricato M, Li X, Hratchian HP, Izmaylov AF, Bloino J, Zheng G, Sonnenberg JL, Hada M, Ehara M, Toyota K, Fukuda R, Hasegawa J, Ishida M, Nakajima T, Honda Y, Kitao O, Nakai H, Vreven T, Montgomery JAJr, Peralta JE, Ogliaro F, Bearpark M, Heyd JJ, Brothers E, Kudin KN, Staroverov VN, Kobayashi R, Normand J, Raghavachari K, Rendell A, Burant JC, Iyengar SS, Tomasi J, Cossi M, Rega N, Millam JM, Klene M, Knox JE, Cross JB, Bakken V, Adamo C, Jaramillo J, Gomperts R, Stratmann RE, Yazyev O, Austin AJ, Cammi R, Pomelli C, Ochterski JW, Martin RL, Morokuma K, Zakrzewski VG, Voth GA, Salvador P, Dannenberg JJ, Dapprich S, Daniels AD, Farkas Ö, Foresman JB, Ortiz JV, Cioslowski J, Fox DJ. *Gaussian 09W (Revision A.1)*, Gaussian Inc.: Wallingford, CT, 2009.

**Table 1.** Optical Properties of Studied Compounds in THF.

Sample	$\lambda^a_{\text{max}}(\text{nm})$	$\lambda^b_{\text{emis}}(\text{nm})$	$\epsilon (\text{M}^{-1} \text{cm}^{-1})$	$\Phi_{\text{fluo}}^d$	Stokes Shift (nm)	FWHM (nm)	$\sigma_2^c$ (GM)
<b>4a</b>	650	682	84600	0.019	32	48	-
<b>4b</b>	659	693	77800	0.028	34	51	-
<b>4c</b>	658	690	66000	0.032	32	49	-
<b>4d</b>	667	699	60700	0.043	32	53	-
<b>5a</b>	645	685	75500	<0.001	40	51	347
<b>5b</b>	651	685	45900	0.002	34	55	218
<b>5c</b>	651	685	59300	0.001	34	52	444
<b>5d</b>	657	685	39100	0.002	28	59	610

<sup>a</sup>The peak wavelength of absorption spectra

<sup>b</sup> The peak wavelength of one-photon fluorescence with excitation wavelength  $\lambda_{\text{abs}}$

<sup>c</sup> TPA cross section at wavelength of 800 nm

<sup>d</sup> Rhodamine was used as a standard for fluorescence quantum yields

**Table 2.** Selected parameters for the vertical excitation (UV-Vis absorption and fluorescence emission) of the compounds. Electronic excitation energies (eV) and oscillator strengths ( $f$ ), configurations of the low-lying excited states of 5a and its fluorescent precursors. THF was employed as solvent in the calculation. Calculated by **B3LYP/6-31G(d)/ LANL2DZ**, based on the optimized ground state geometries.

Electronic		TDDFT/B3LYP/6-31G(d)			
		Excitation energy	$f^b$	Composition <sup>c</sup>	CI <sup>d</sup>
Absorption	S <sub>0</sub> →S <sub>1</sub>	2.13eV (581 nm)	0.7053	H→L	0.8445
	S <sub>0</sub> →S <sub>3</sub>	2.50eV (495 nm)	0.2551	H-2→L	0.7047
	S <sub>0</sub> →S <sub>15</sub>	4.48eV (277 nm)	0.3739	H→L+1	0.6525
Triplet	S <sub>0</sub> →T <sub>1</sub>	0.98eV (1267 nm)	0.0000 <sup>e</sup>	H→L	0.7153
	S <sub>0</sub> →T <sub>2</sub>	1.98eV (627 nm)	0.0000	H-1→L	0.6896
	S <sub>0</sub> →T <sub>3</sub>	2.07eV (599 nm)	0.0000	H-2→L+1	0.6884

<sup>a</sup> Only selected excited states were considered. The numbers in parentheses are the excitation energy in wavelength. <sup>b</sup> Oscillator strength. <sup>c</sup> H stands for HOMO and L stands for LUMO. Only the main configurations are presented. <sup>d</sup> Coefficient of the wave function for each excitations. The CI coefficients are in absolute values. <sup>e</sup> No spin-orbital coupling effect was considered, thus the  $f$  values are zero.

**Table 3.** Electronic Excitation Energies (eV), Corresponding Oscillator Strengths ( $f$ ), Main Configurations and CI Coefficients of the Low-Lying Electronic Excited States of the 4a. Calculated by **TDDFT//B3LYP/6-31G(D)/LanL2DZ** Based on the Optimized Ground State Geometries

Electronic transition	TDDFT//B3LYP/6-31G(d)			
	Energy <sup>a</sup> (eV/nm)	$f^b$	Composition <sup>c</sup>	CI <sup>d</sup>
S <sub>0</sub> →S <sub>1</sub>	2.05 / 605	0.8462	H→L	0.7082
S <sub>0</sub> →S <sub>2</sub>	2.51 / 493	0.0098	H-1→L	0.6996
S <sub>0</sub> →S <sub>3</sub>	2.61 / 474	0.3454	H-2→L	0.7027
S <sub>0</sub> →S <sub>8</sub>	3.32 / 374	0.1977	H-7→L	0.6791
			H-5→L	0.1299
			H→L+1	0.1171
			H-18→L	0.1519
S <sub>0</sub> →S <sub>23</sub>	3.79 / 327	0.1301	H-16→L	0.4603
			H-13→L	0.1567
			H-3→L+1	0.4788
S <sub>0</sub> →S <sub>14</sub>	4.26 / 291	0.7034	H→L+1	0.5444
			H→L+3	0.4282
S <sub>0</sub> →S <sub>21</sub>	5.08 / 244	0.2227	H-12→L	0.1165
			H-2→L+2	0.1865
			H-1→L+1	0.6218
			H-1→L+3	0.2173
T <sub>0</sub> →T <sub>1</sub>	0.90 / 1378	0.0000 <sup>e</sup>	H→L	0.7205
T <sub>0</sub> →T <sub>2</sub>	2.06 / 602	0.0000 <sup>e</sup>	H-1→L	0.6879
T <sub>0</sub> →T <sub>3</sub>	2.14 / 580	0.0000 <sup>e</sup>	H-2→L	0.6850

<sup>a</sup>Only the selected low-lying/excited states are presented. <sup>b</sup>Oscillator strength. <sup>c</sup>Only the main configurations are presented. <sup>d</sup>The CI coefficients are in absolute values. <sup>e</sup>No spin-orbital coupling effect was considered, thus the  $f$  values are zero.

## Figure Captions

**Figure 1.** Normalized absorption spectra of studied compounds in THF ( $1 \times 10^{-5} \text{M}$ ). The inset shows the shifts of maximum absorption wavelengths.

**Figure 2.** Fluorescence spectra of studied compounds in THF ( $1 \times 10^{-5} \text{M}$ ).

**Figure 3.** Femtosecond transient absorption spectra of (a) **4a** (b) **5a** compounds in THF.

**Figure 4.** Transient absorption spectra with different time delays for (a) **4a** (b) **5a** compounds. The excitation wavelengths are peak maximums of absorption spectrums.

**Figure 5.** (a) The position effect of heavy atom on transient absorption spectra at 650 nm probe wavelength. The figure inset indicates molecular structure of compounds. Femtosecond transient absorption spectra as a function of time of (b) **4a** and (c) **5a**.

**Figure 6.** Effects of different number of heavy atoms on transient absorption spectra which are probed at bleach wavelength. The figure inset indicates molecular structure of compounds.

**Figure 7.** Electron density maps of the frontier molecular orbitals of compound **4a** based on the optimized ground state geometry. The solvent THF was considered in the calculations (PCM model). Calculated at the B3LYP/6-31G(d)/LanL2DZ level with Gaussian 09W.

**Figure 8.** Selected frontier molecular orbitals involved in the excitation, emission and triplet excited states of **5a**. ISC stands for intersystem crossing. The calculations are at the B3LYP/6-31G(d)/LANL2DZ level using Gaussian 09W.

**Figure 9.** Spin density of the compounds **4a** and **5a**. Calculated based on the optimized triplet state by DFT at the B3LYP/6-31G(d)/LanL2DZ level using Gaussian 09W.

**Figure 10.** Experimental results (symbols) and theoretical fits (solid line) of open aperture Z-scan experiments for **5a-d** compounds at  $80 \text{ GW/cm}^2$  input intensity in THF, using 800 nm femtosecond pulses.

Fig. 1

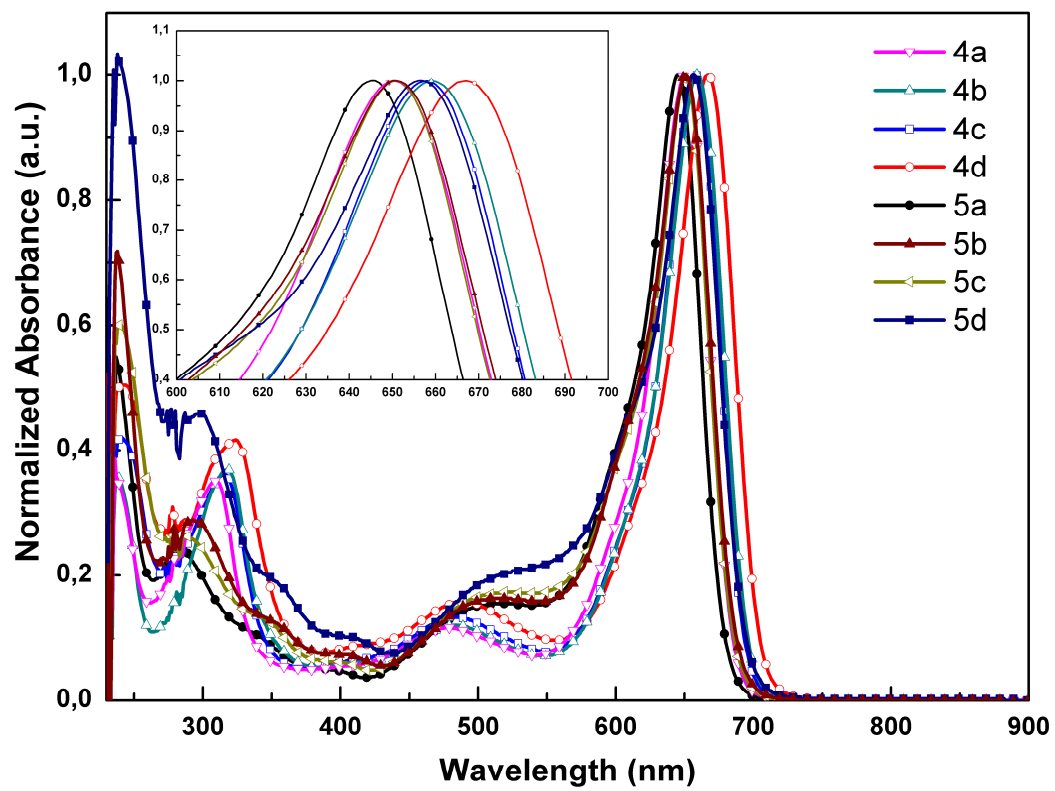


Fig.2

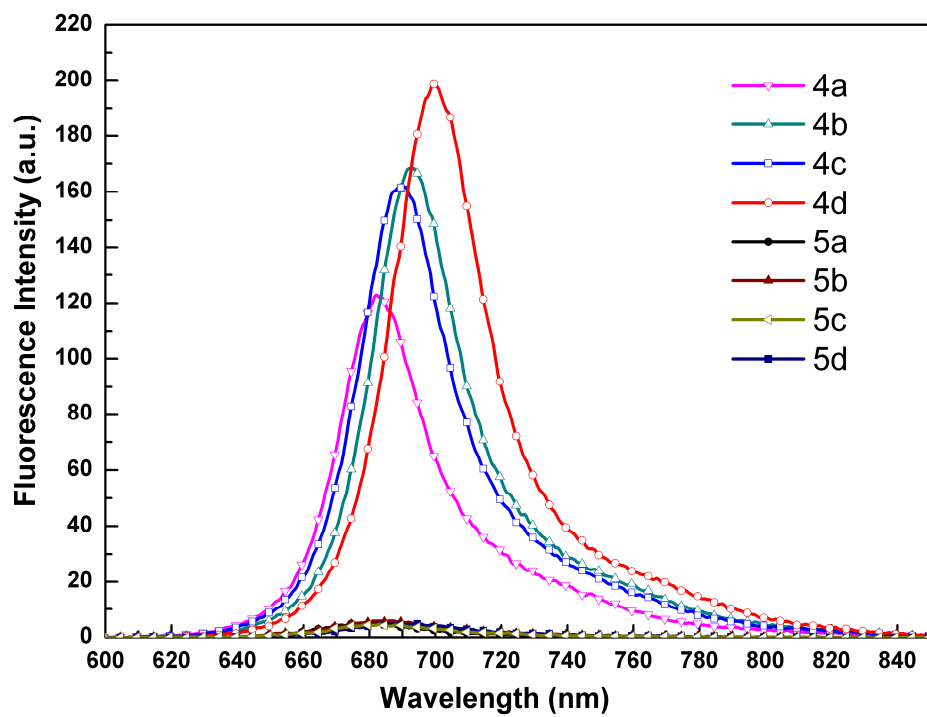


Fig. 3

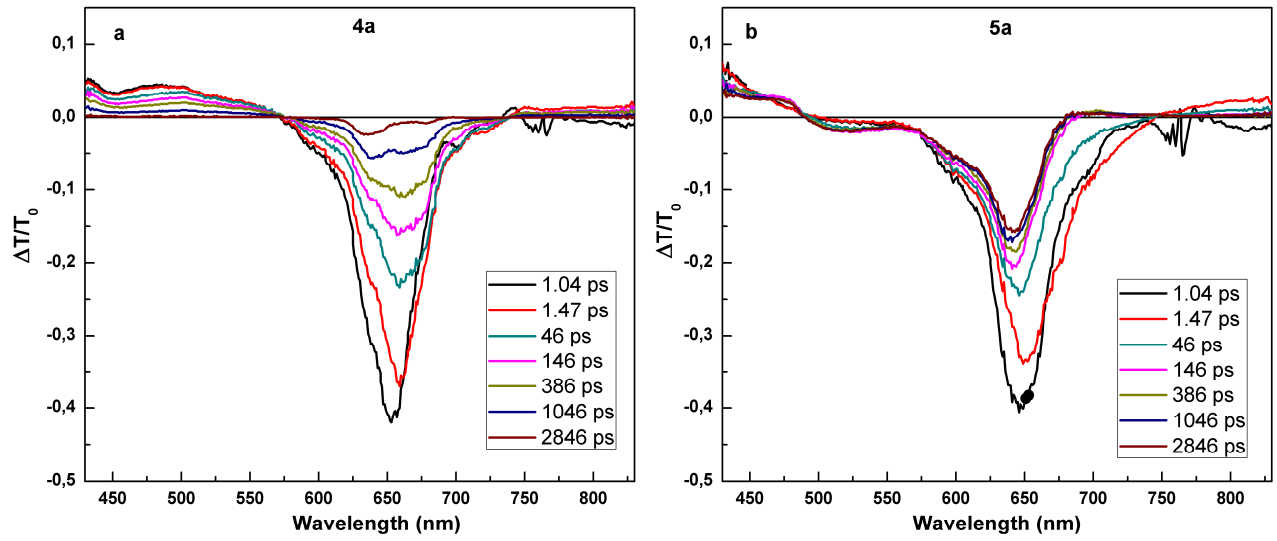


Fig. 4

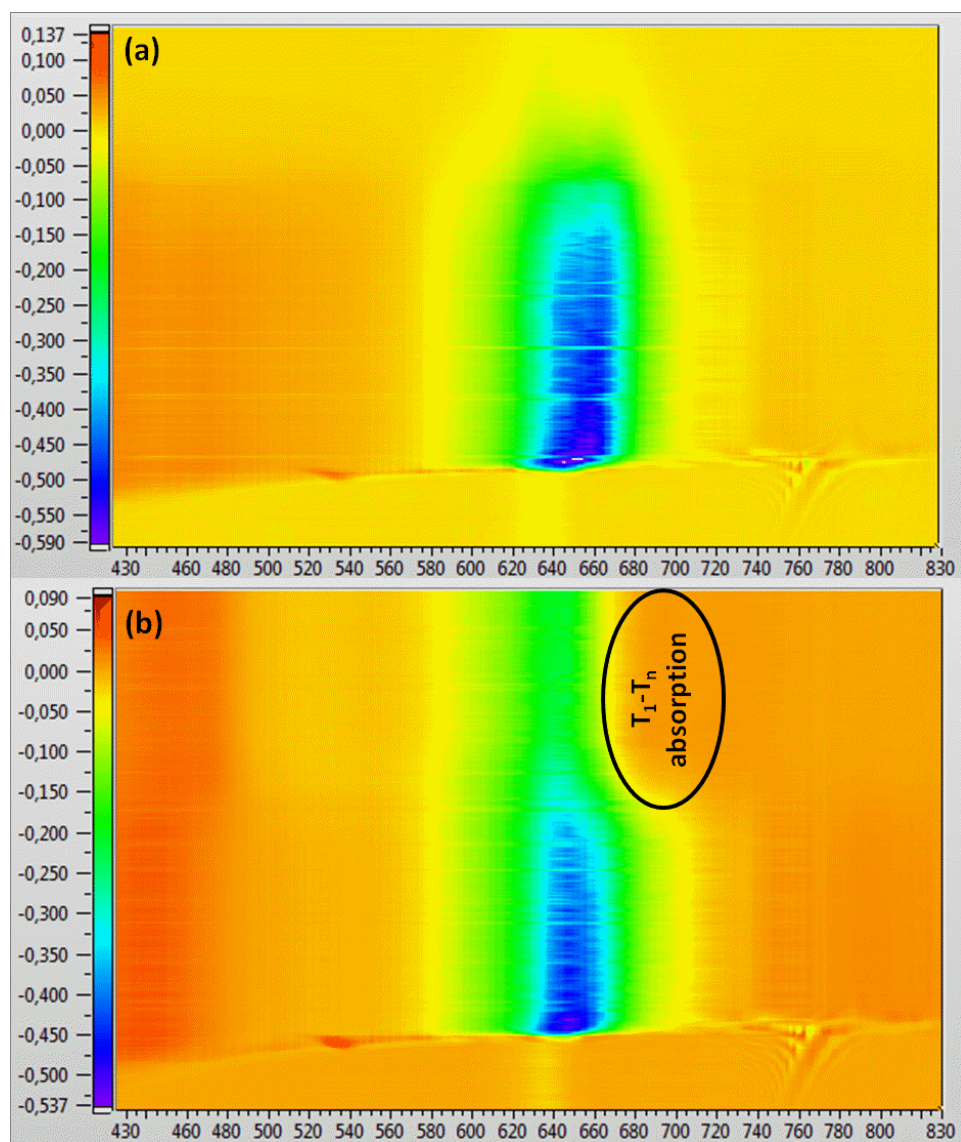


Fig. 5

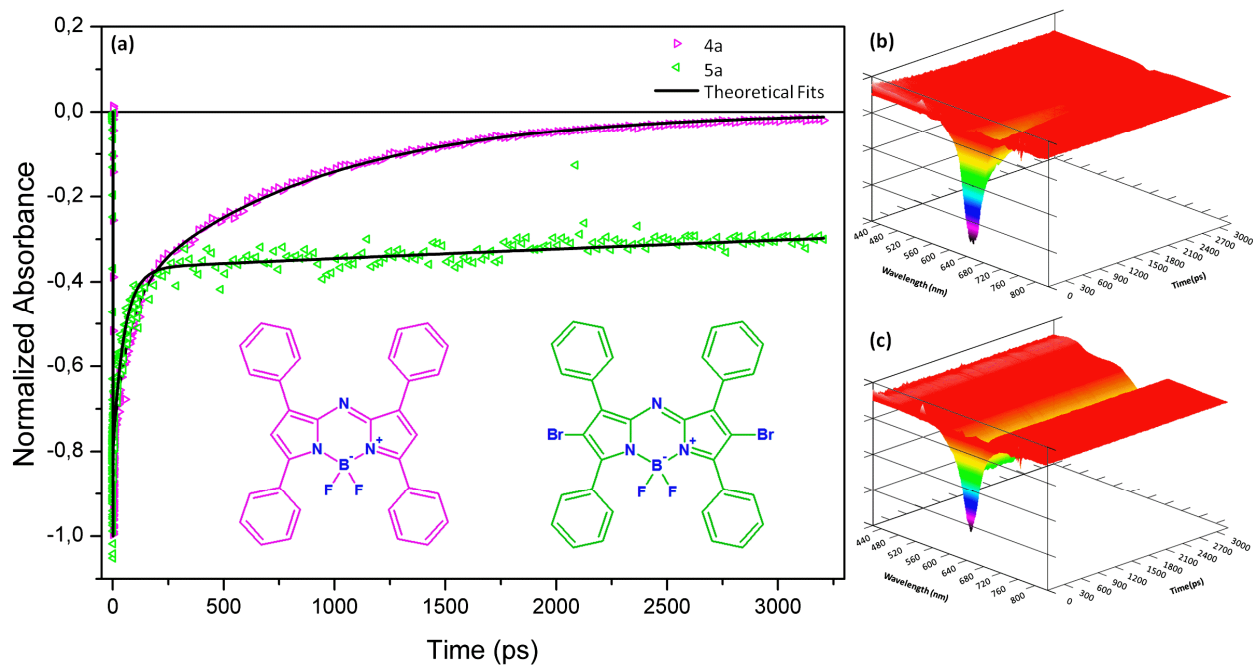


Fig. 6

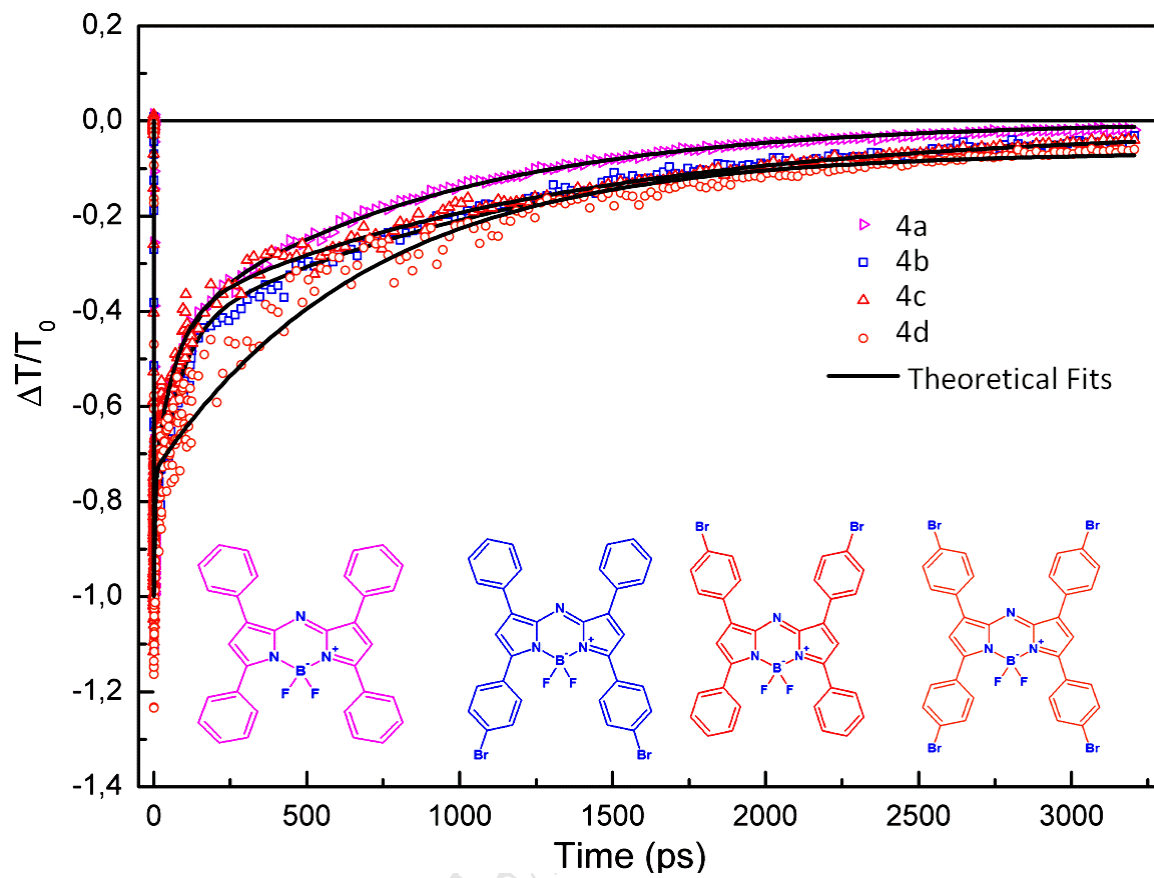


Fig. 7

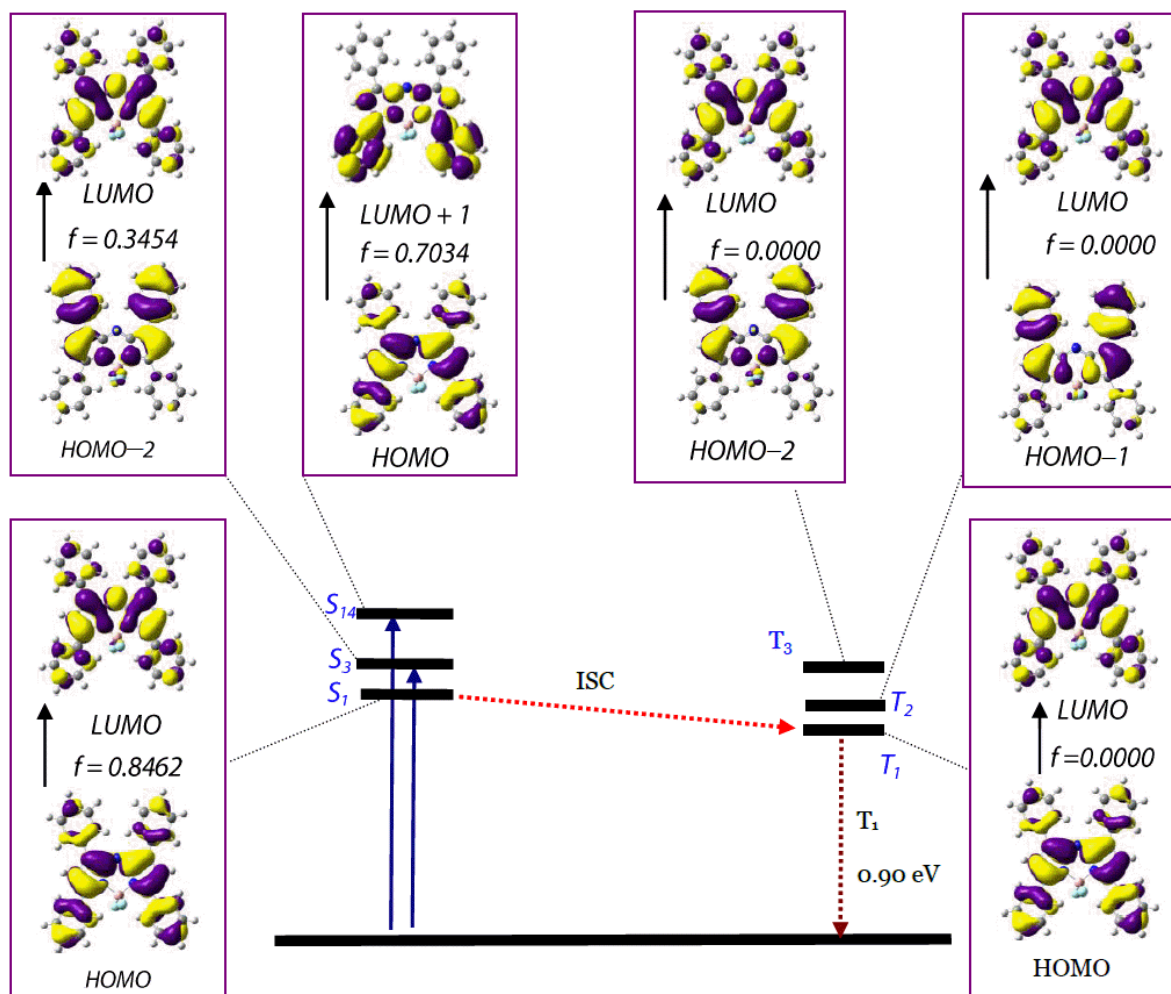


Fig. 8

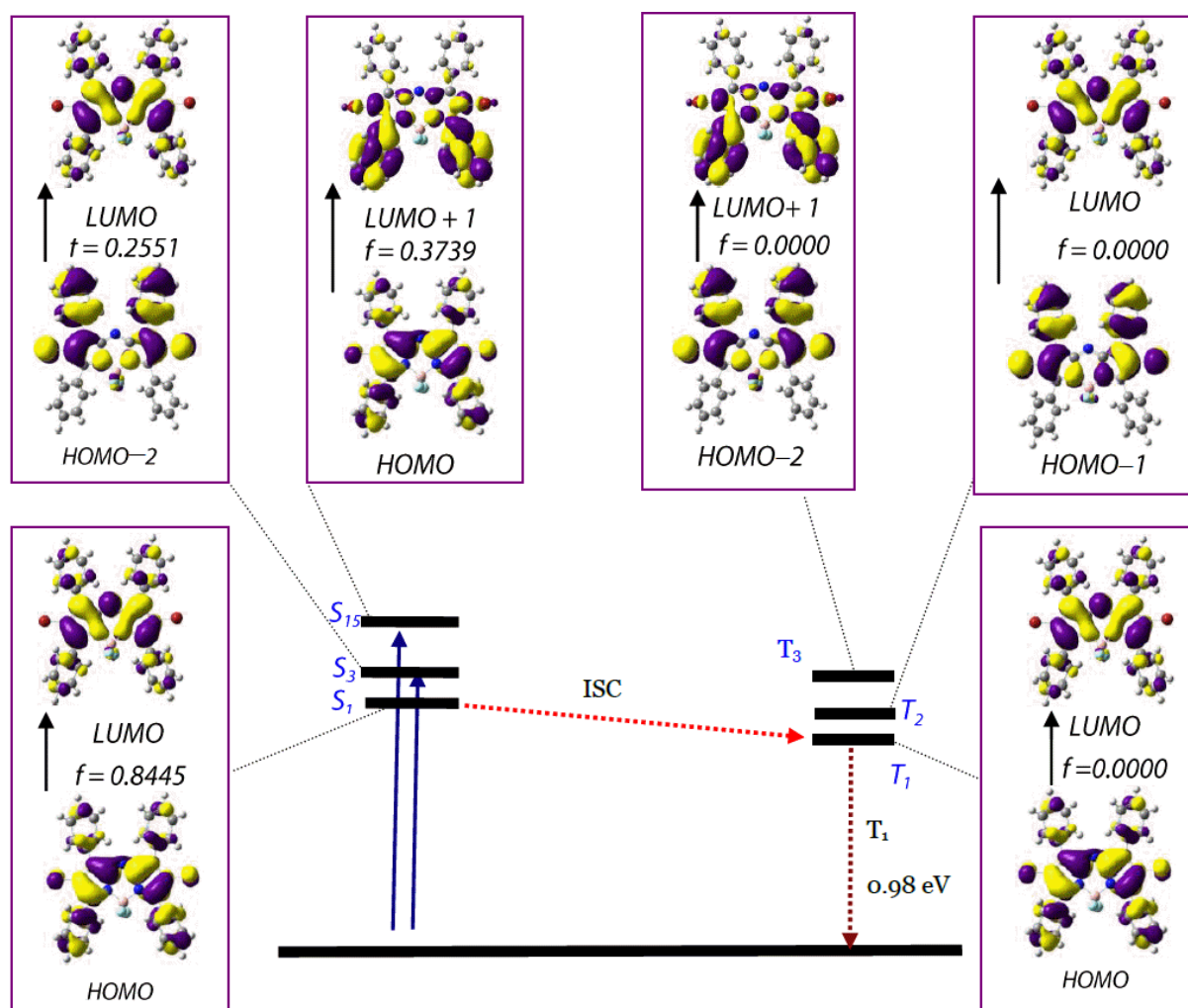


Fig. 9

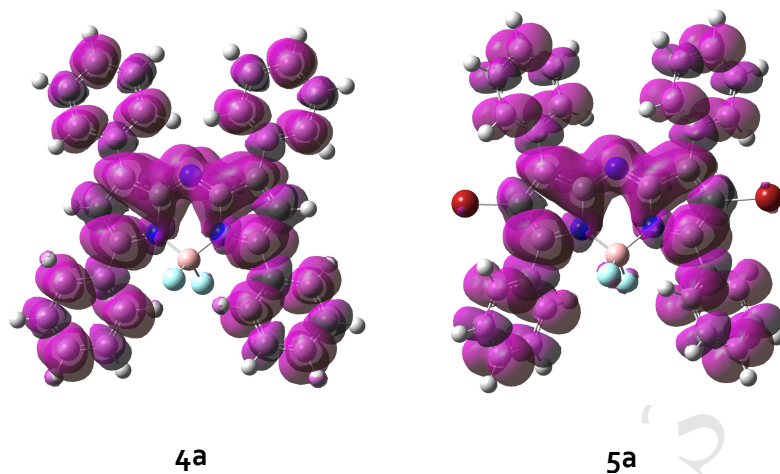
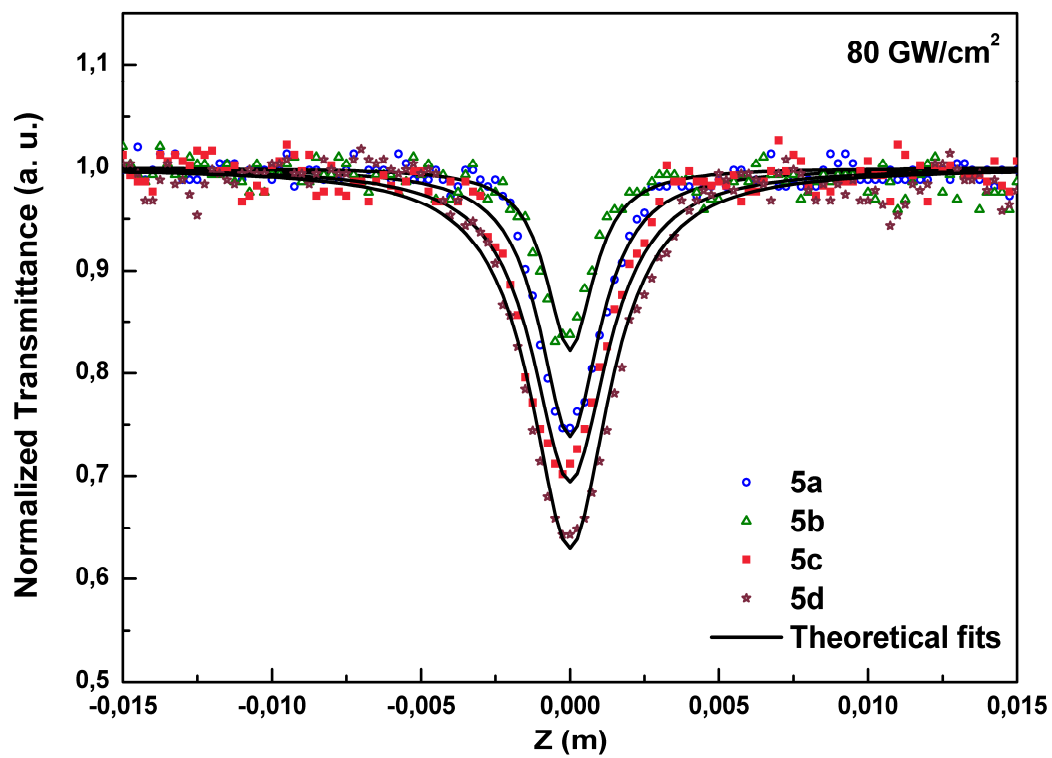
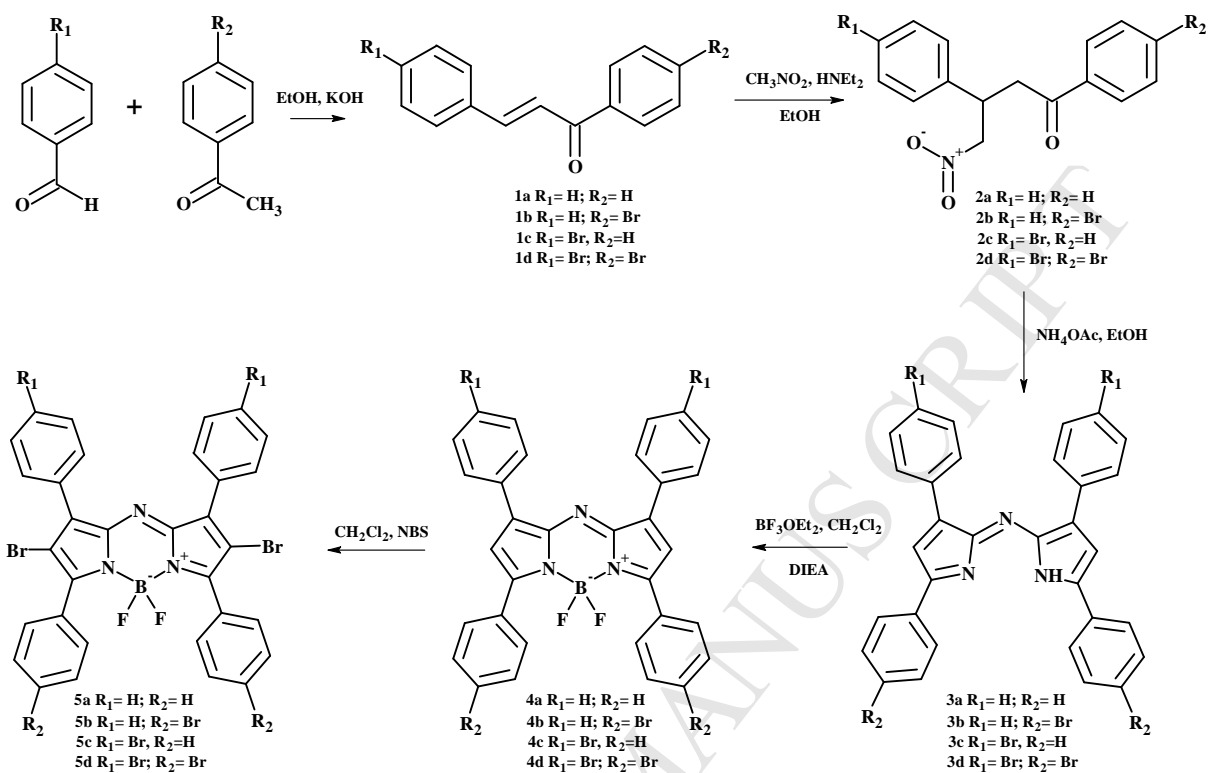


Fig. 10





Scheme 1. Synthesis of the aza-BODIPY Compounds (4a-d, 5a-d)

**Highlights**

- The effects of heavy atom to two photon absorption for Aza-BODIPY
- The effect of the number and position of heavy atom on intersystem crossing.
- Two photon absorption properties of Aza-BODIPY compounds for photodynamic therapy

## Supporting Information

# The Effect of Heavy Atom to Two Photon Absorption Properties and Intersystem Crossing Mechanism in Aza-Boron-Dipyrromethene Compounds

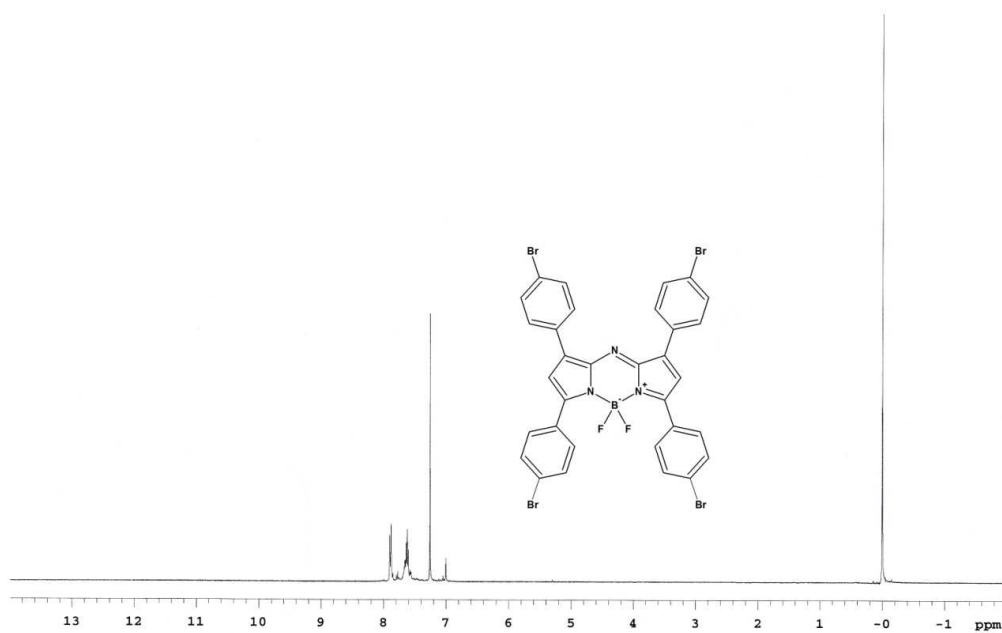
Ahmet Karatay,<sup>a</sup> M. Ceren Miser,<sup>b</sup> Xiaoneng Cui,<sup>c</sup> Betül Küçüköz,<sup>a</sup> Halil Yılmaz,<sup>b</sup> Gökhan Sevinç,<sup>b</sup> Elif Akhüseyin,<sup>a</sup> Xueyan Wu,<sup>c</sup> Mustafa Hayvali,<sup>\*b</sup> H. Gul Yaglioglu,<sup>\*a</sup> Jianzhang Zhao,<sup>c</sup> Ayhan Elmali<sup>a</sup>

<sup>a</sup> Department of Engineering Physics, Faculty of Engineering, Ankara University, 06100 Beşevler, Ankara, Turkey

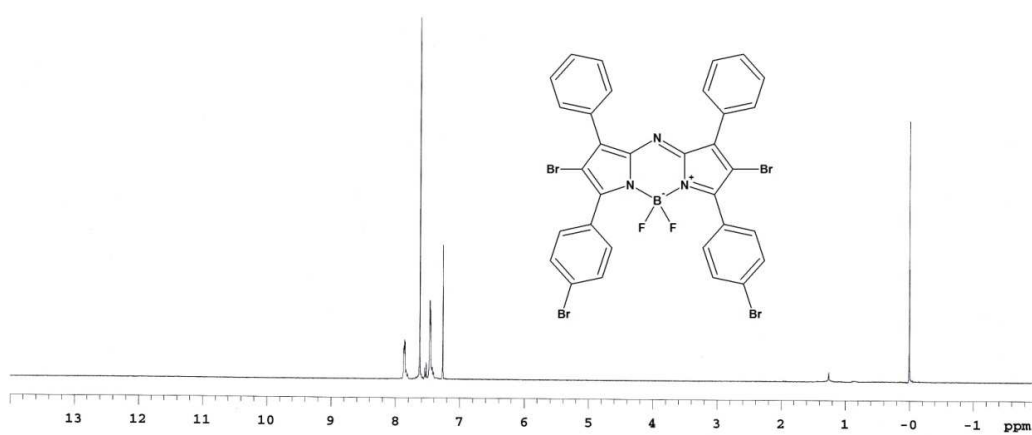
<sup>b</sup> Department of Chemistry, Faculty of Science, Ankara University, 06100 Beşevler, Ankara, Turkey

<sup>c</sup> Dalian University of Technology, State Key Laboratory of Fine Chemicals, School of Chemical Engineering, E-208 West Campus, 2 Ling-Gong Road, Dalian 116024, P. R. China

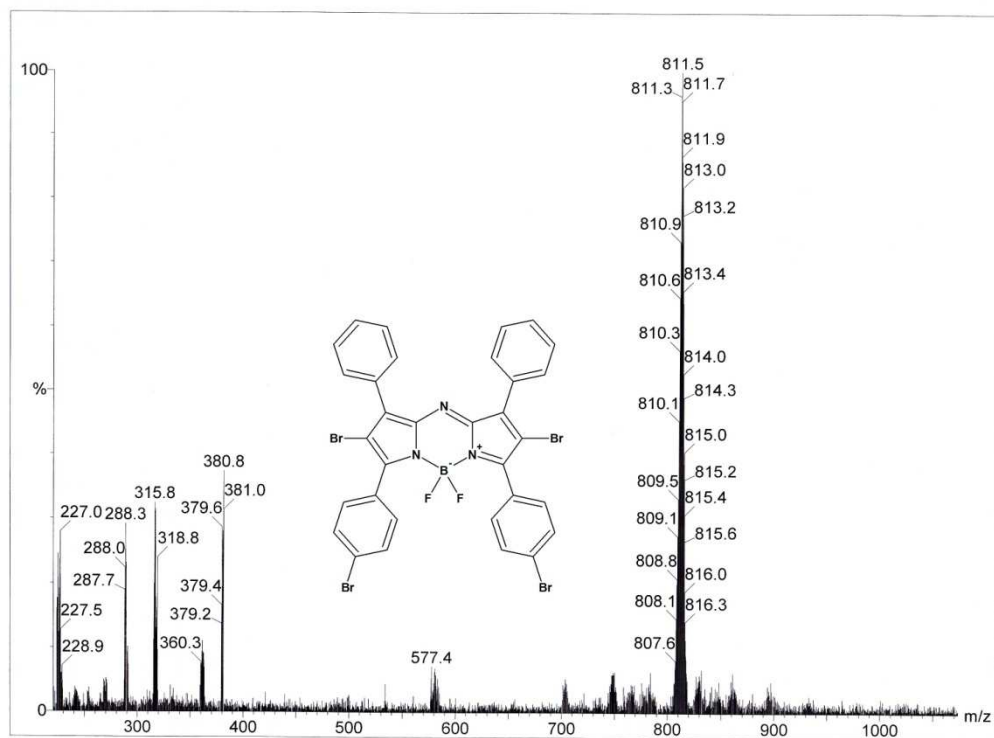
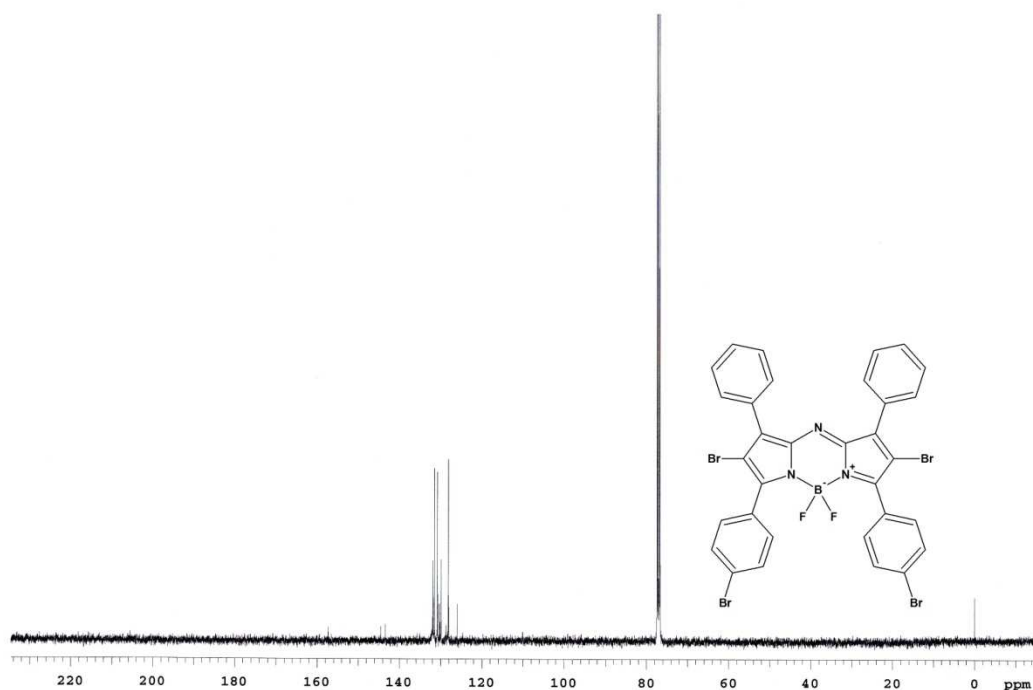
## 1. SYNTHESIS AND CHARACTERIZATION



**Figure S1.** <sup>1</sup>H NMR spectra of the compound **4d** in CD<sub>3</sub>Cl



**Figure S2.** <sup>1</sup>H NMR spectra of the compound **5b** in CD<sub>3</sub>Cl



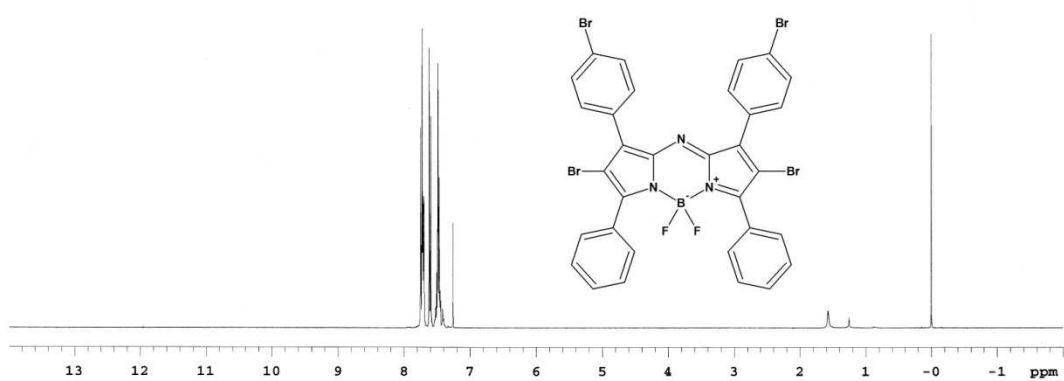


**Figure S5.**  $^1\text{H}$  NMR spectra of the compound **5c** in  $\text{CD}_3\text{Cl}$

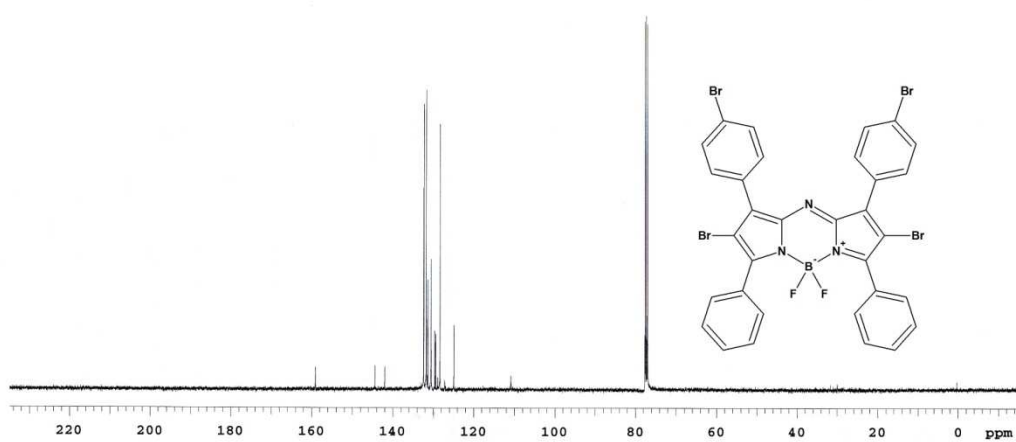


**Figure S6.**  $^{13}\text{C}$  NMR spectra of the compound **5c** in  $\text{CD}_3\text{Cl}$

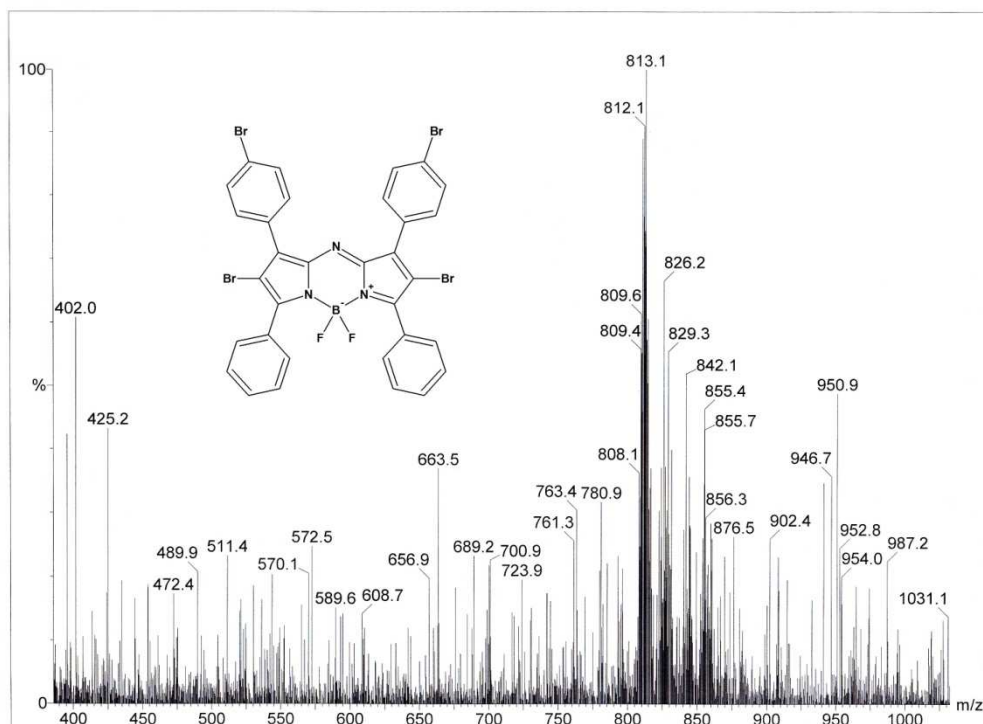


Figure S7. LC-MS spectra of the compound **5c**

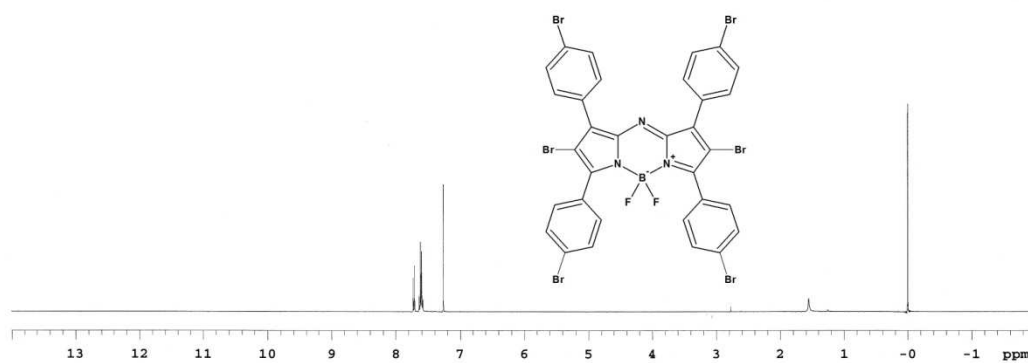
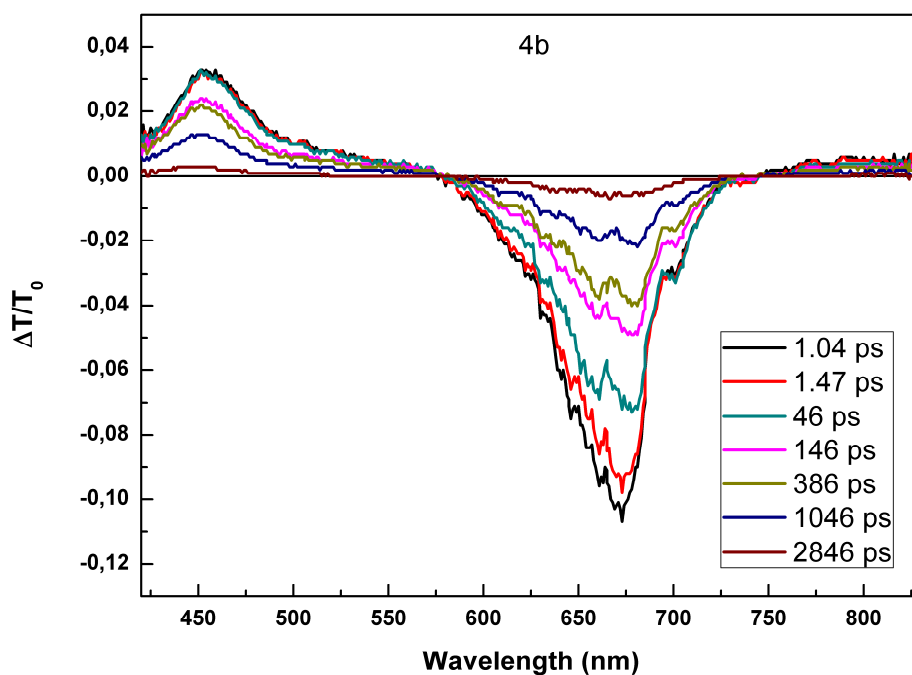
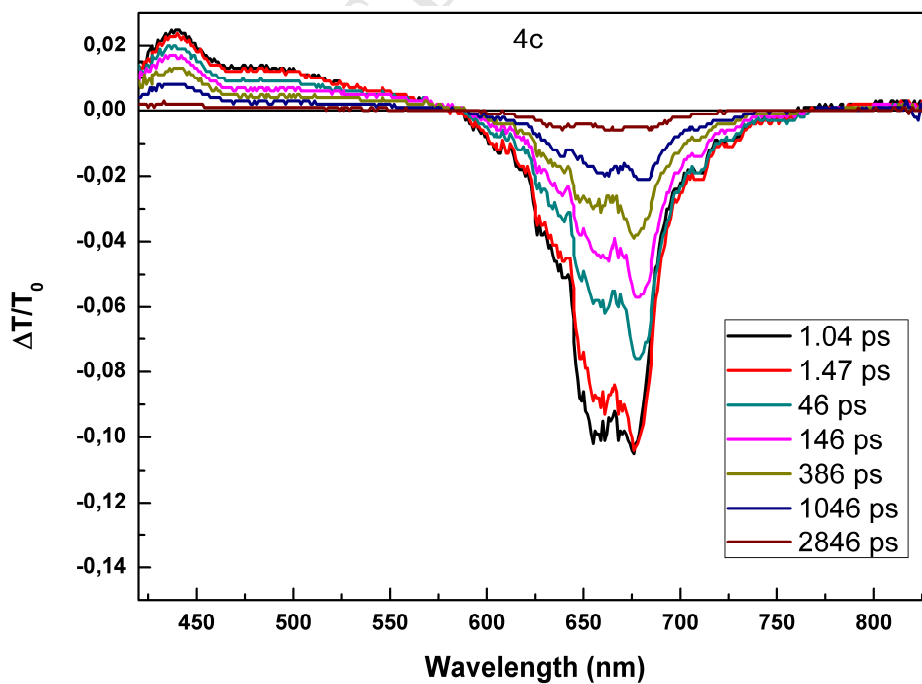


Figure S8. <sup>1</sup>H NMR spectra of the compound **5d** in CD<sub>3</sub>Cl

## 2. ULTRAFAST PUMP PROBE SPECTROSCOPY



**Figure S9.** Transient absorption spectra of **4b** compound with different time delays



**Figure S10.** Transient absorption spectra of **4c** compound with different time delays

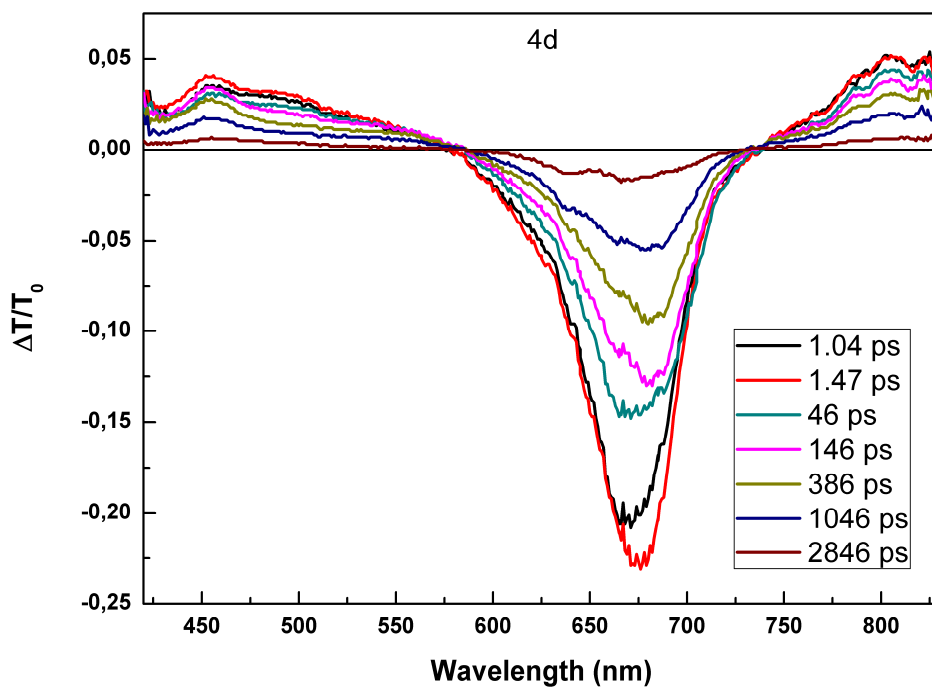


Figure S11. Transient absorption spectra of **4d** compound with different time delays

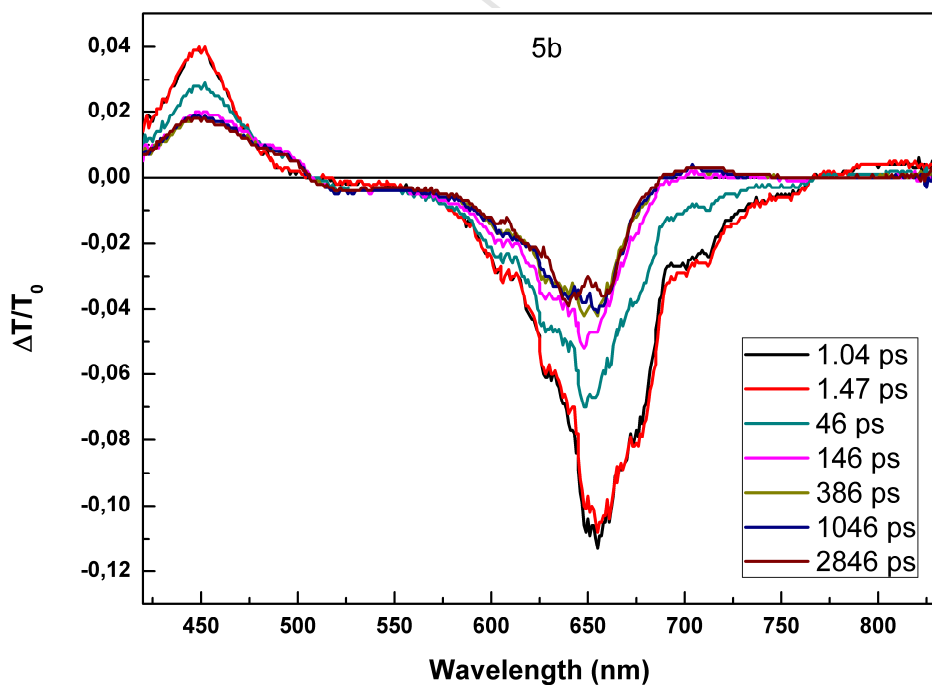


Figure S12. Transient absorption spectra of **5b** compound with different time delays

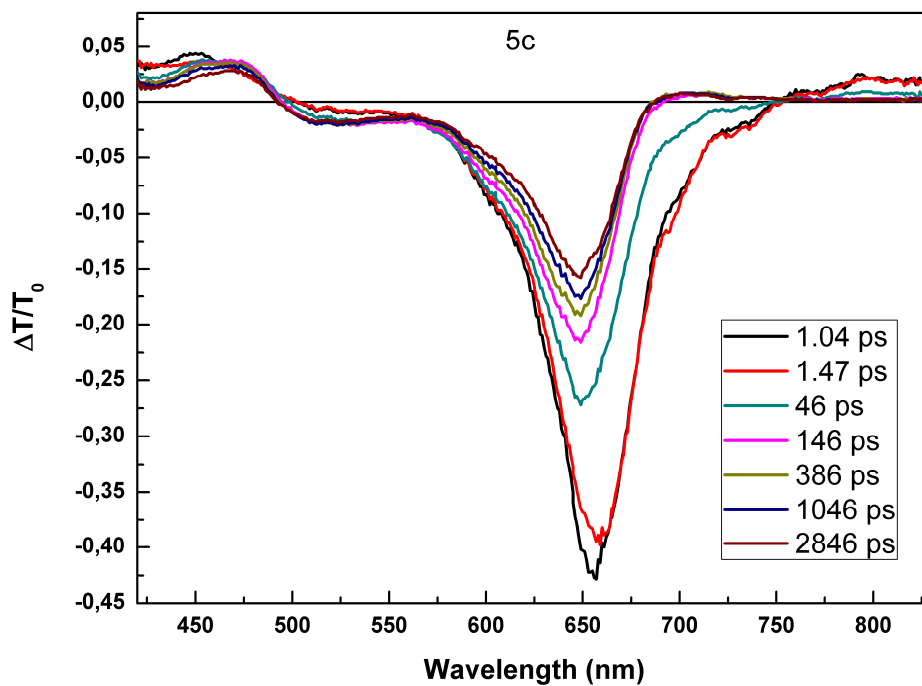


Figure S13. Transient absorption spectra of **5c** compound with different time delays

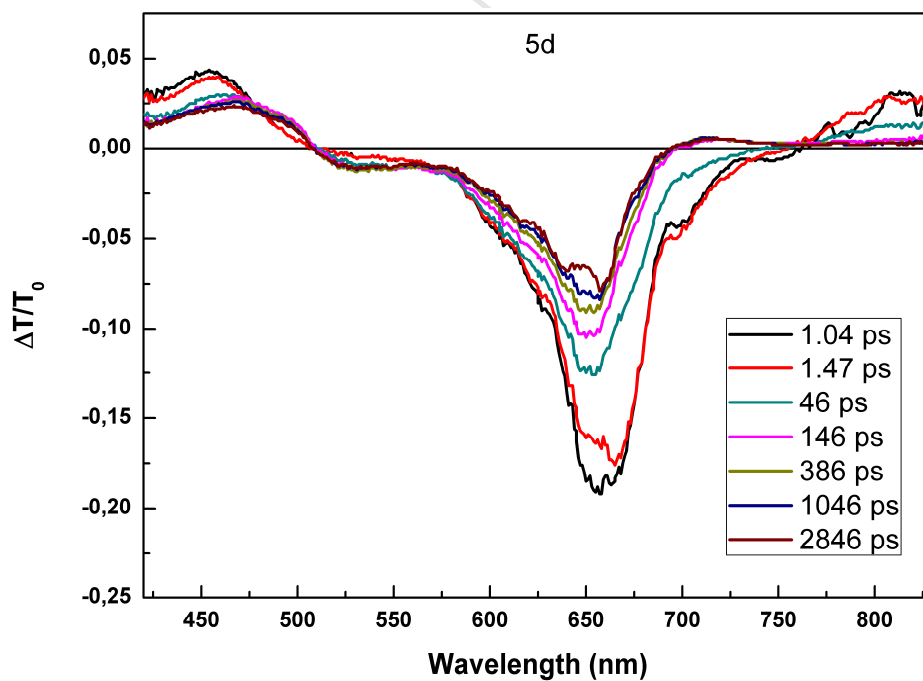
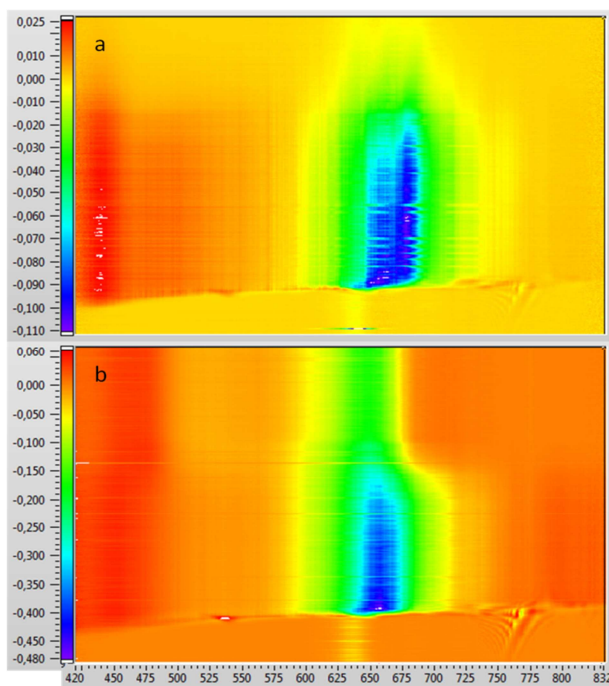
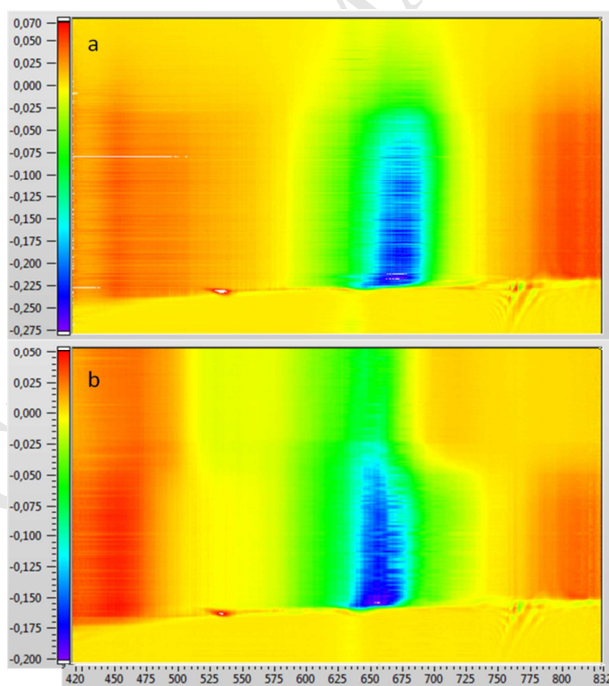


Figure S14. Transient absorption spectra of **5d** compound with different time delays



**Figure S15.** Transient absorption spectra of (a) **4c** and (b) **5c** compounds with different time delays



**Figure S16.** Transient absorption spectra of (a) **4d** and (b) **5d** compounds with different time delays

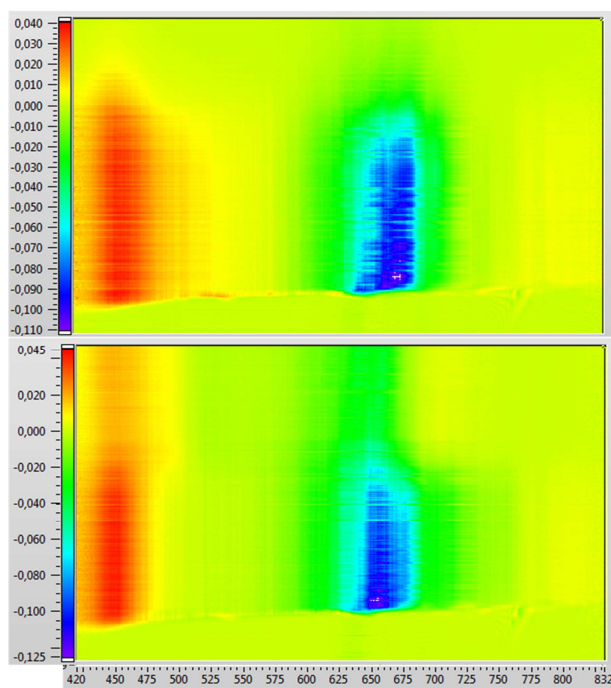


**Figure S17.** Transient absorption spectra of (a) **4b** and (b) **5b** compounds with different time delays

## 3. DFT CALCULATION

**Table S1.** Electronic Excitation Energies (Ev), Corresponding Oscillator Strengths ( $f$ ), Main Configurations and CI Coefficients of the Low-Lying Electronic Excited States of the **4a**. Calculated by TDDFT//B3LYP/6-31G(D)/LanL2DZ Based on the Optimized Ground State Geometries

Electronic transition	TDDFT//B3LYP/6-31G(d)			
	Energy <sup>a</sup> (eV/nm)	$f^b$	Composition <sup>c</sup>	CI <sup>d</sup>
S <sub>0</sub> →S <sub>1</sub>	2.05 / 605	0.8462	H→L	0.7082
S <sub>0</sub> →S <sub>2</sub>	2.51 / 493	0.0098	H-1→L	0.6996
S <sub>0</sub> →S <sub>3</sub>	2.61 / 474	0.3454	H-2→L	0.7027
S <sub>0</sub> →S <sub>8</sub>	3.32 / 374	0.1977	H-7→L	0.6791
			H-5→L	0.1299
			H→L+1	0.1171
			H-18→L	0.1519
S <sub>0</sub> →S <sub>23</sub>	3.79 / 327	0.1301	H-16→L	0.4603
			H-13→L	0.1567
			H-3→L+1	0.4788
S <sub>0</sub> →S <sub>14</sub>	4.26 / 291	0.7034	H→L+1	0.5444
			H→L+3	0.4282
S <sub>0</sub> →S <sub>21</sub>	5.08 / 244	0.2227	H-12→L	0.1165
			H-2→L+2	0.1865
			H-1→L+1	0.6218
			H-1→L+3	0.2173
T <sub>0</sub> →T <sub>1</sub>	0.899 / 1378	0.0000 <sup>e</sup>	H→L	0.7205
T <sub>0</sub> →T <sub>2</sub>	2.06 / 602	0.0000 <sup>e</sup>	H-1→L	0.6879
T <sub>0</sub> →T <sub>3</sub>	2.14 / 580	0.0000 <sup>e</sup>	H-2→L	0.6850

<sup>a</sup> Only the selected low-lying excited states are presented. <sup>b</sup> Oscillator strength. <sup>c</sup> Only the main configurations are presented. <sup>d</sup> The CI coefficients are in absolute values. <sup>e</sup> No spin-orbital coupling effect was considered, thus the  $f$  values are zero.

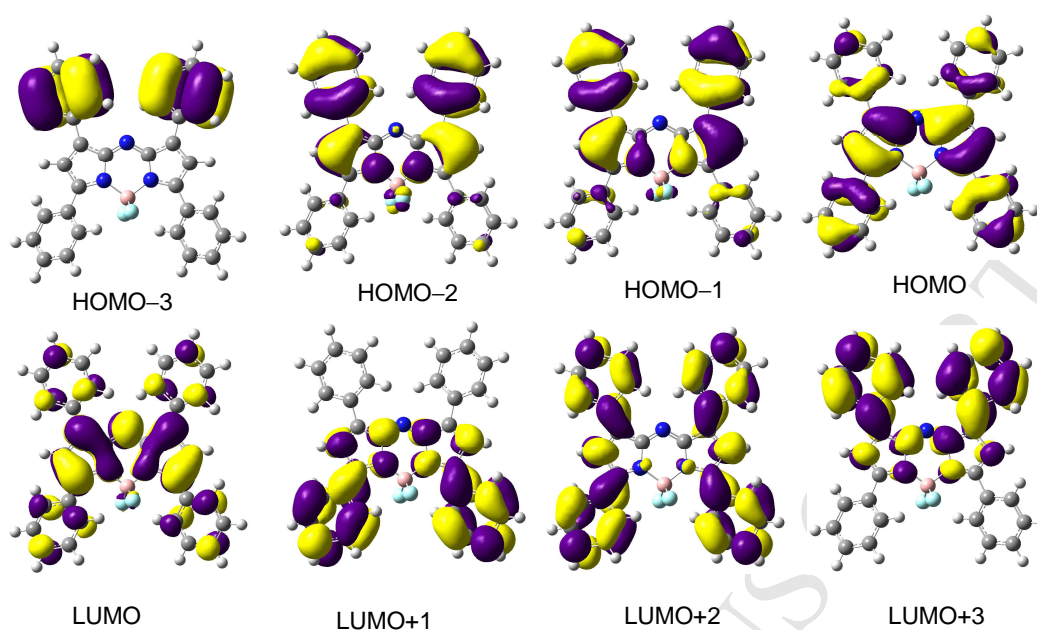


**Figure S18.** Electron density maps of the frontier molecular orbitals of compound **4a** based on the optimized ground state geometry. The solvent THF was considered in the calculations (PCM model). Calculated at the B3LYP/6-31G(d)/LanL2DZ level with Gaussian 09W.

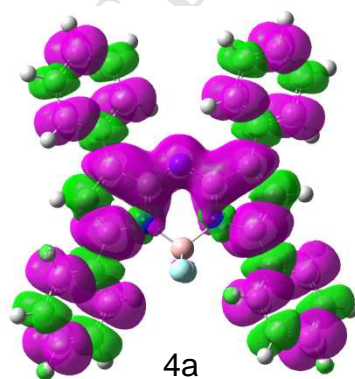


**Figure S19.** Spin density of the compound **4a**. Calculated based on the optimized triplet state by DFT at the B3LYP/6-31G(d)/LanL2DZ level using Gaussian 09W.

**Table S2.** Electronic Excitation Energies (Ev), Corresponding Oscillator Strengths ( $f$ ), Main Configurations and CI Coefficients of the Low-Lying Electronic Excited States of the **4b**. Calculated by TDDFT//B3LYP/6-31G(D)/LanL2DZ Based on the Optimized Ground State Geometries

Electronic transition	TDDFT//B3LYP/6-31G(d)			
	Energy <sup>a</sup> (eV/nm)	$f^b$	Composition <sup>c</sup>	CI <sup>d</sup>
S <sub>0</sub> →S <sub>1</sub>	2.02 / 616	0.8861	H→L	0.7078
S <sub>0</sub> →S <sub>2</sub>	2.46 / 503	0.0151	H-1→L	0.6998
S <sub>0</sub> →S <sub>3</sub>	2.56 / 484	0.3956	H-2→L	0.7026
S <sub>0</sub> →S <sub>6</sub>	3.15 / 393	0.2235	H-4→L	0.4953
			H-3→L	0.4858
			H→L+1	0.1011
S <sub>0</sub> →S <sub>13</sub>	4.12 / 301	0.5975	H-13→L	0.1702
			H-11→L	0.1914
			H→L+1	0.6189
S <sub>0</sub> →S <sub>26</sub>	4.92 / 252	0.1311	H→L+3	0.1651
			H-2→L+2	0.1501
			H-1→L+1	0.6513
			H-1→L+3	0.1053
T <sub>0</sub> →T <sub>1</sub>	0.894 / 1386	0.0000 <sup>e</sup>	H→L+8	0.1423
			H→L	0.7188
			H-1→L	0.6863
T <sub>0</sub> →T <sub>2</sub>	2.02 / 613	0.0000 <sup>e</sup>	H-1→L	0.6863
T <sub>0</sub> →T <sub>3</sub>	2.10 / 592	0.0000 <sup>e</sup>	H-2→L	0.6831

<sup>a</sup> Only the selected low-lying excited states are presented. <sup>b</sup> Oscillator strength. <sup>c</sup> Only the main configurations are presented. <sup>d</sup> The CI coefficients are in absolute values. <sup>e</sup> No spin-orbital coupling effect was considered, thus the  $f$  values are zero.

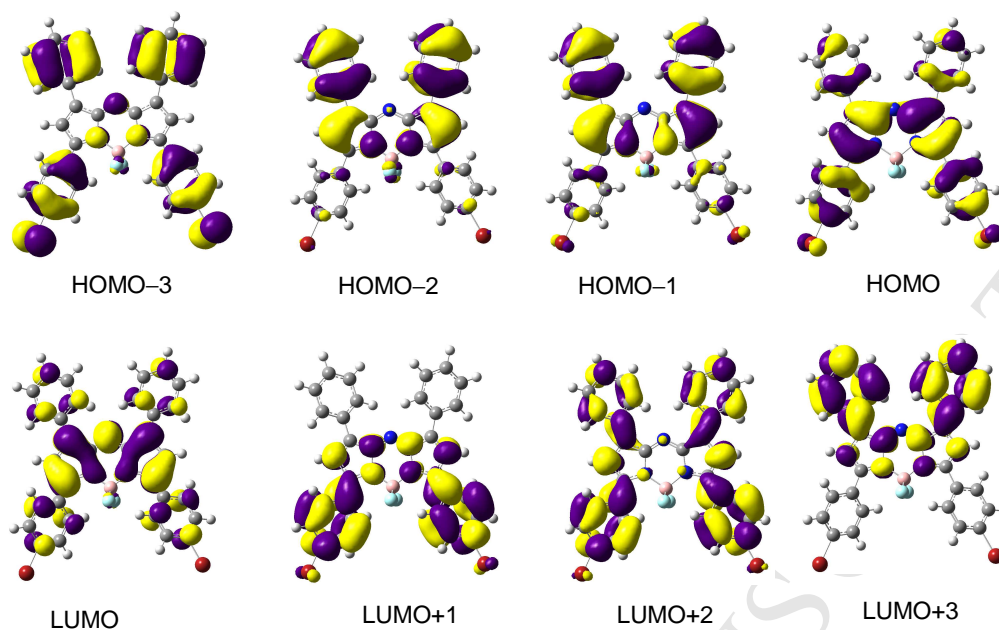
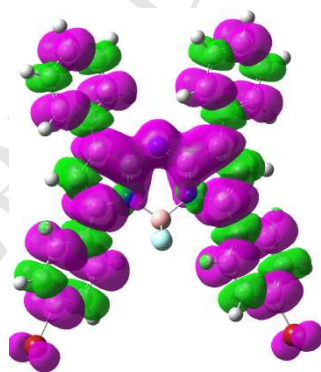


**Figure S20.** Electron density maps of the frontier molecular orbitals of compound **4b** based on the optimized ground state geometry. The solvent THF was considered in the calculations (PCM model). Calculated at the B3LYP/6-31G(d)/LanL2DZ level with Gaussian 09W.



**4b**

**Figure S21.** Spin density of the compound **4b**. Calculated based on the optimized triplet state by DFT at the B3LYP/6-31G(d)/LanL2DZ level using Gaussian 09W.

**Table S3.** Electronic Excitation Energies (Ev), Corresponding Oscillator Strengths ( $f$ ), Main Configurations and CI Coefficients of the Low-Lying Electronic Excited States of the **4c**. Calculated by TDDFT//B3LYP/6-31G(D)/LanL2DZ Based on the Optimized Ground State Geometries

Electronic transition	TDDFT//B3LYP/6-31G(d)			
	Energy <sup>a</sup> (eV/nm)	$f^b$	Composition <sup>c</sup>	CI <sup>d</sup>
S <sub>0</sub> →S <sub>1</sub>	2.01 / 614	0.8613	H→L	0.7073
S <sub>0</sub> →S <sub>2</sub>	2.49 / 497	0.0083	H-1→L	0.6975
S <sub>0</sub> →S <sub>3</sub>	2.58 / 480	0.4123	H-2→L	0.7026
S <sub>0</sub> →S <sub>6</sub>	3.26 / 381	0.2160	H-5→L	0.6818
			H-3→L	0.1027
			H→L+3	0.1085
S <sub>0</sub> →S <sub>13</sub>	4.14 / 300	0.4870	H→L+1	0.6655
			H→L+3	0.2236
S <sub>0</sub> →S <sub>17</sub>	4.32 / 287	0.3246	H-5→L	0.1093
			H→L+1	0.2060
			H→L+3	0.6430
			H→L+4	0.1150
S <sub>0</sub> →S <sub>27</sub>	5.00 / 248	0.5936	H-1→L+1	0.6378
			H-1→L+3	0.2534
T <sub>0</sub> →T <sub>1</sub>	0.884 / 1403	0.0000 <sup>e</sup>	H→L	0.7202
T <sub>0</sub> →T <sub>2</sub>	2.05 / 604	0.0000 <sup>e</sup>	H-9→L	0.1006
			H-8→L	0.1159
			H-1→L	0.6797
T <sub>0</sub> →T <sub>3</sub>	2.13 / 581	0.0000 <sup>e</sup>	H-10→L	0.1441
			H-2→L	0.6770

<sup>a</sup> Only the selected low-lying excited states are presented. <sup>b</sup> Oscillator strength. <sup>c</sup> Only the main configurations are presented. <sup>d</sup> The CI coefficients are in absolute values. <sup>e</sup> No spin-orbital coupling effect was considered, thus the  $f$  values are zero.

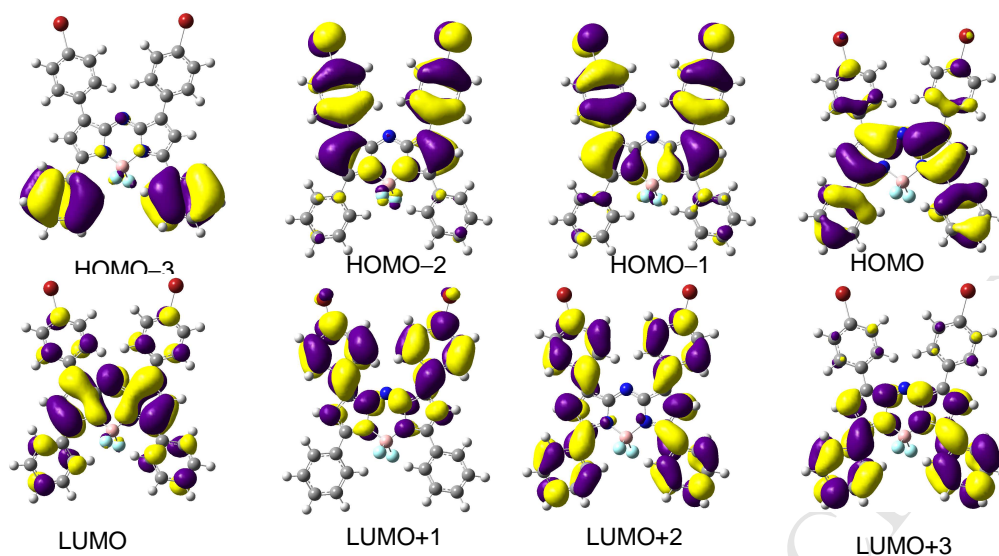


**Figure S22.** Electron density maps of the frontier molecular orbitals of compound **4c** based on the optimized ground state geometry. The solvent THF was considered in the calculations (PCM model). Calculated at the B3LYP/6-31G(d)/LanL2DZ level with Gaussian 09W.

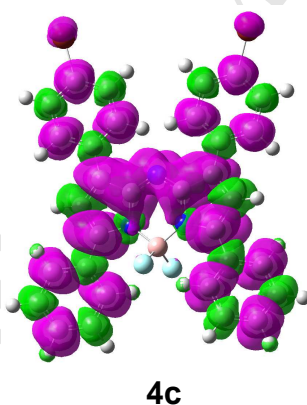


**Figure S23.** Spin density of the compound **4c**. Calculated based on the optimized triplet state by DFT at the B3LYP/6-31G(d)/LanL2DZ level using Gaussian 09W.

**Table S4.** Electronic Excitation Energies (Ev), Corresponding Oscillator Strengths ( $f$ ), Main Configurations and CI Coefficients of the Low-Lying Electronic Excited States of the **4d**. Calculated by TDDFT//B3LYP/6-31G(D)/LanL2DZ Based on the Optimized Ground State Geometries

Electronic transition	TDDFT//B3LYP/6-31G(d)			
	Energy <sup>a</sup> (eV/nm)	$f^b$	Composition <sup>c</sup>	CI <sup>d</sup>
S <sub>0</sub> →S <sub>1</sub>	2.07 / 599	0.8610	H→L	0.7020
S <sub>0</sub> →S <sub>2</sub>	2.33 / 533	0.0099	H-1→L	0.6983
S <sub>0</sub> →S <sub>3</sub>	2.41 / 514	0.3446	H-2→L	0.7037
S <sub>0</sub> →S <sub>4</sub>	2.88 / 431	0.1858	H-3→L	0.7001
S <sub>0</sub> →S <sub>21</sub>	4.36 / 284	0.4710	H-17→L	0.3612
			H→L+1	0.4775
			H→L+2	0.1920
			H→L+3	0.2907
T <sub>0</sub> →T <sub>1</sub>	0.964 / 1286	0.0000 <sup>e</sup>	H-10→L	0.1070
			H→L	0.7109
T <sub>0</sub> →T <sub>2</sub>	1.93 / 642	0.0000 <sup>e</sup>	H-10→L	0.1323
			H-1→L	0.6787
T <sub>0</sub> →T <sub>3</sub>	2.01 / 615	0.0000 <sup>e</sup>	H-9→L	0.1516
			H-2→L	0.6778

<sup>a</sup> Only the selected low-lying excited states are presented. <sup>b</sup> Oscillator strength. <sup>c</sup> Only the main configurations are presented. <sup>d</sup> The CI coefficients are in absolute values. <sup>e</sup> No spin-orbital coupling effect was considered, thus the  $f$  values are zero.

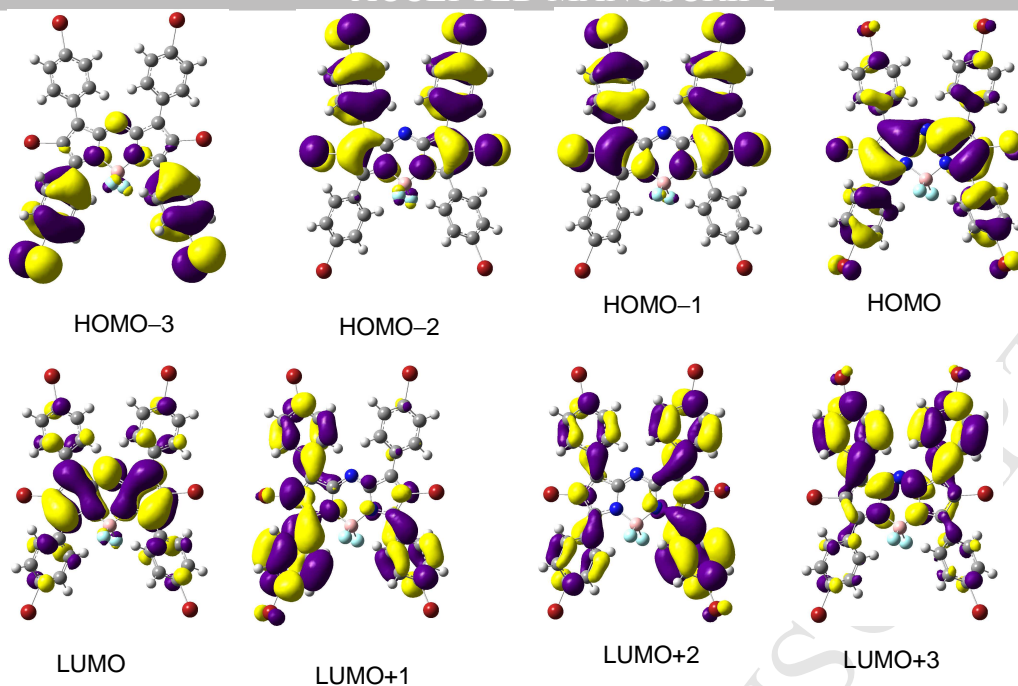


**Figure S24.** Electron density maps of the frontier molecular orbitals of compound **4d** based on the optimized ground state geometry. The solvent THF was considered in the calculations (PCM model). Calculated at the B3LYP/6-31G(d)/LanL2DZ level with Gaussian 09W.

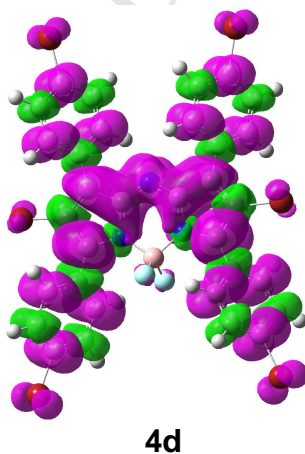


**Figure S25.** Spin density of the compound **4d**. Calculated based on the optimized triplet state by DFT at the B3LYP/6-31G(d)/LanL2DZ level using Gaussian 09W.

**Table S5.** Selected parameters for the vertical excitation (UV-vis absorption and fluorescence emission) of the compounds. Electronic excitation energies (eV) and oscillator strengths ( $f$ ), configurations of the low-lying excited states of **5a** and its fluorescent precursors. THF was employed as solvent in the calculation. Calculated by B3LYP/6-31G(d)/ LANL2DZ, based on the optimized ground state geometries.

Electronic		TDDFT/B3LYP/6-31G(d)			
		Excitation	$f^b$	Composition <sup>c</sup>	CI <sup>d</sup>
Absorption	$S_0 \rightarrow S_1$	2.13 eV (581)	0.7053	H→L	0.8445
	$S_0 \rightarrow S_3$	2.50 eV (495)	0.2551	H-2→L	0.7047
	$S_0 \rightarrow S_{15}$	4.48eV (277)	0.3739	H→L+1	0.6525
Triplet	$S_0 \rightarrow T_1$	0.98 eV (1267)	0.0000 <sup>e</sup>	H→L	0.7153
	$S_0 \rightarrow T_2$	1.98 eV (627)	0.0000	H-1 →L	0.6896
	$S_0 \rightarrow T_3$	2.07 eV (599)	0.0000	H-2→L+1	0.6884

<sup>a</sup> Only selected excited states were considered. The numbers in parentheses are the excitation energy in wavelength. <sup>b</sup> Oscillator strength. <sup>c</sup> H stands for HOMO and L stands for LUMO. Only the main configurations are presented. <sup>d</sup> Coefficient of the wave function for each excitations. The CI coefficients are in absolute values. <sup>e</sup> No spin-orbital coupling effect was considered, thus the  $f$  values are zero.

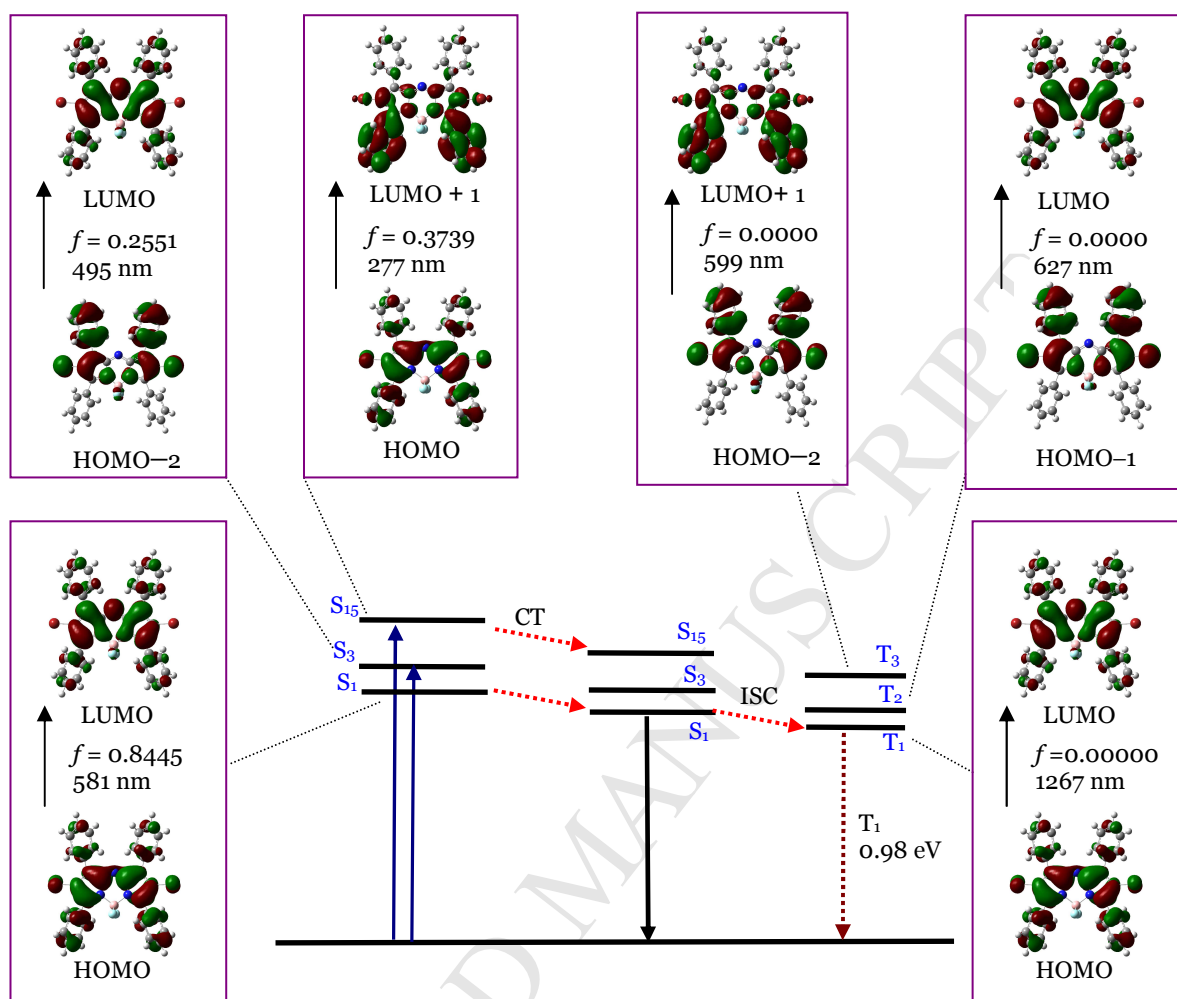


**Figure S26.** Selected frontier molecular orbitals involved in the excitation, emission and triplet excited states of **5a**. CT stands for conformation transformation. The calculations are at the B3LYP/6-31G(d)/LANL2DZ level using Gaussian 09W.

**Table S6.** Selected parameters for the vertical excitation (UV-vis absorption and fluorescence emission) of the compounds. Electronic excitation energies (eV) and oscillator strengths ( $f$ ), configurations of the low-lying excited states of **5b** and its fluorescent precursors. THF was employed as solvent in the calculation. Calculated by B3LYP/6-31G(d)/ LANL2DZ, based on the optimized ground state geometries.

Electronic		TDDFT/B3LYP/6-31G(d)			
		Excitation	$f^b$	Composition <sup>c</sup>	CI <sup>d</sup>
Absorption	$S_0 \rightarrow S_1$	2.11 eV (589)	0.8629	H→L	0.7040
	$S_0 \rightarrow S_3$	2.46 eV (505)	0.2847	H-2→L	0.7046
	$S_0 \rightarrow S_{17}$	4.33eV (286)	0.3894	H→L+1	0.6475
Triplet	$S_0 \rightarrow T_1$	0.98 eV (1268)	0.0000 <sup>e</sup>	H→L	0.7124
	$S_0 \rightarrow T_2$	1.94 eV (638)	0.0000	H-1 → L	0.6893
	$S_0 \rightarrow T_3$	2.03 eV (611)	0.0000	H-2→L	0.6876

<sup>a</sup> Only selected excited states were considered. The numbers in parentheses are the excitation energy in wavelength. <sup>b</sup> Oscillator strength. <sup>c</sup> H stands for HOMO and L stands for LUMO. Only the main configurations are presented. <sup>d</sup> Coefficient of the wave function for each excitations. The CI coefficients are in absolute values. <sup>e</sup> No spin-orbital coupling effect was considered, thus the  $f$  values are zero.

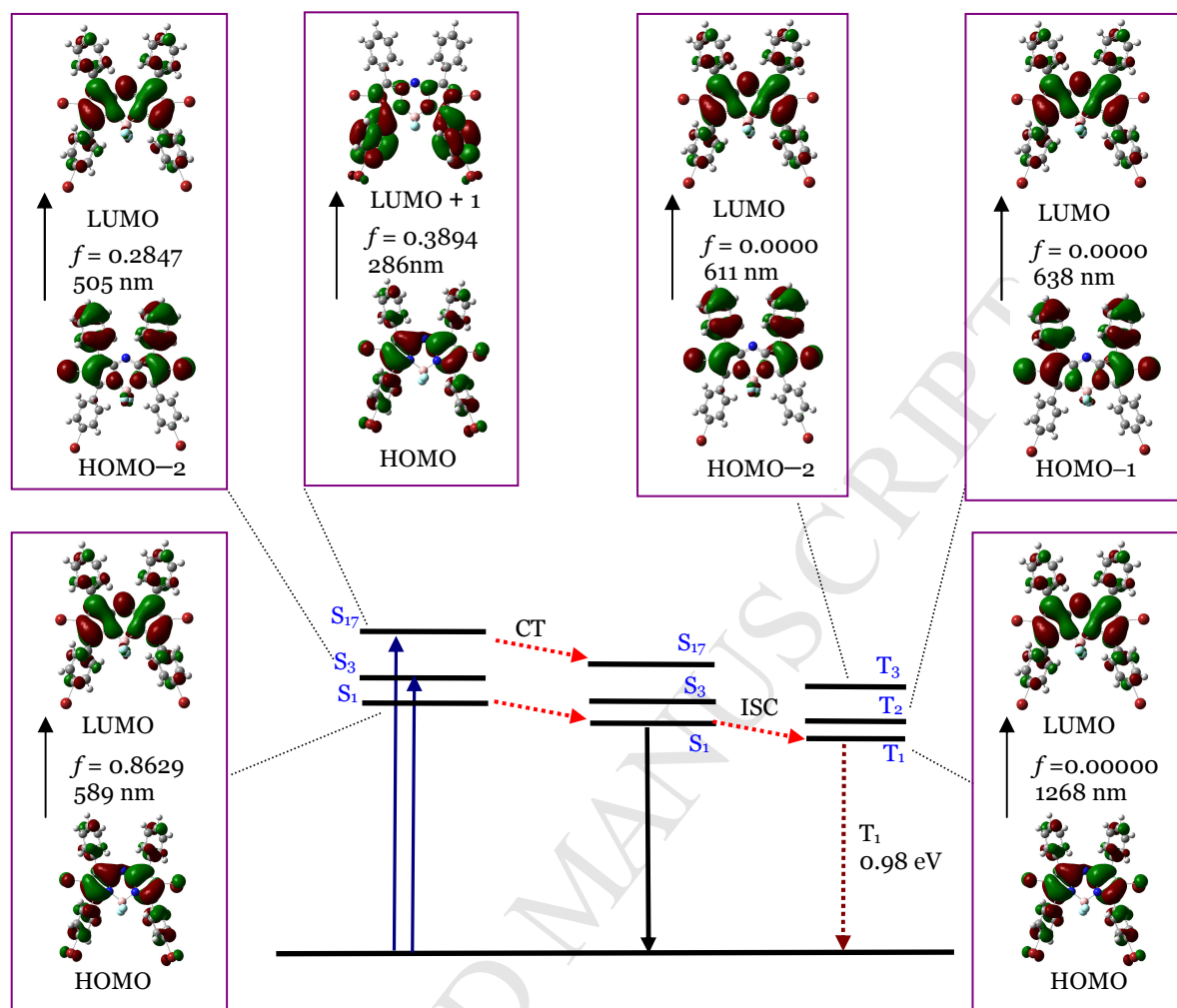


**Figure S27.** Selected frontier molecular orbitals involved in the excitation, emission and triplet excited states of **5b**. CT stands for conformation transformation. The calculations are at the B3LYP/6-31G(d)/LANL2DZ level using Gaussian 09W.

**Table S8.** Selected parameters for the vertical excitation (UV-vis absorption and fluorescence emission) of the compounds. Electronic excitation energies (eV) and oscillator strengths ( $f$ ), configurations of the low-lying excited states of **5c** and its fluorescent precursors. THF was employed as solvent in the calculation. Calculated by B3LYP/6-31G(d)/ LANL2DZ, based on the optimized ground state geometries.

Electronic		TDDFT/B3LYP/6-31G(d)			
		Excitation	$f^b$	Composition <sup>c</sup>	CI <sup>d</sup>
Absorption	$S_0 \rightarrow S_1$	2.10 eV (590)	0.8464	H→L	0.7035
	$S_0 \rightarrow S_3$	2.47 eV (505)	0.3093	H-2→L	0.7037
	$S_0 \rightarrow S_{17}$	4.38eV (283)	0.2372	H→L+1	0.6584
Triplet	$S_0 \rightarrow T_1$	0.96 eV (1287)	0.0000 <sup>e</sup>	H→L	0.7144
	$S_0 \rightarrow T_2$	1.97 eV (630)	0.0000	H-1 → L	0.6797
	$S_0 \rightarrow T_3$	2.05 eV	0.0000	H-2→L	0.6785

<sup>a</sup> Only selected excited states were considered. The numbers in parentheses are the excitation energy in wavelength. <sup>b</sup> Oscillator strength. <sup>c</sup> H stands for HOMO and L stands for LUMO. Only the main configurations are presented. <sup>d</sup> Coefficient of the wave function for each excitations. The CI coefficients are in absolute values. <sup>e</sup> No spin-orbital coupling effect was considered, thus the  $f$  values are zero.

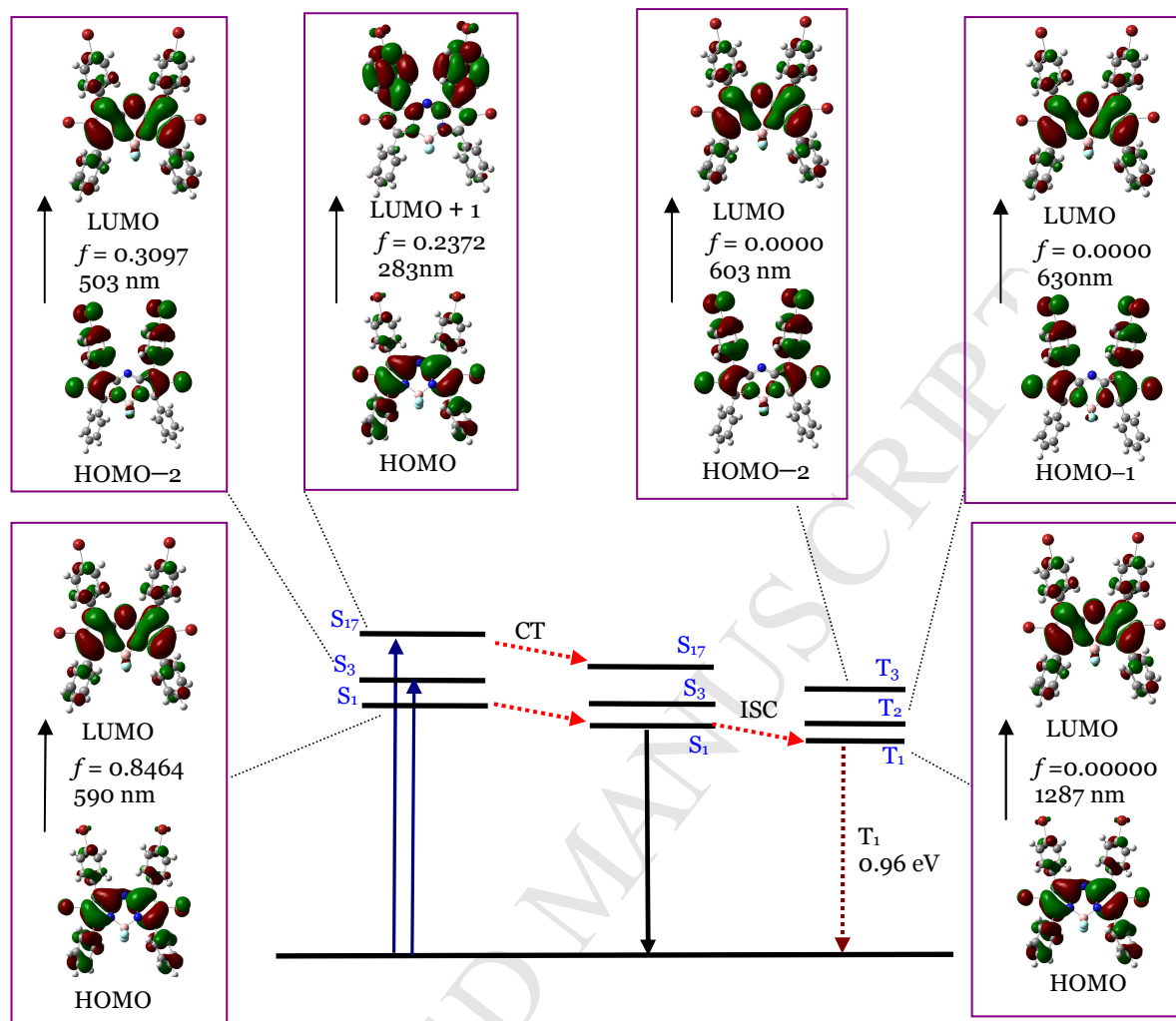


**Figure S28.** Selected frontier molecular orbitals involved in the excitation, emission and triplet excited states of **5c**. CT stands for conformation transformation. The calculations are at the B3LYP/6-31G(d)/LANL2DZ level using Gaussian 09W.

**Table S9.** Selected parameters for the vertical excitation (UV-vis absorption and fluorescence emission) of the compounds. Electronic excitation energies (eV) and oscillator strengths ( $f$ ), configurations of the low-lying excited states of **5d** and its fluorescent precursors. THF was employed as solvent in the calculation. Calculated by B3LYP/6-31G(d)/ LANL2DZ, based on the optimized ground state geometries.

Electronic		TDDFT/B3LYP/6-31G(d)			
		Excitation	$f^b$	Composition <sup>c</sup>	CI <sup>d</sup>
Absorption	$S_0 \rightarrow S_1$	2.07 eV (599)	0.810	H→L	0.7035
	$S_0 \rightarrow S_3$	2.41 eV (514)	0.3446	H-2→L	0.7037
	$S_0 \rightarrow S_{17}$	4.36eV	0.4701	H→L+1	0.4775
Triplet	$S_0 \rightarrow T_1$	0.96eV (nm)	0.0000 <sup>e</sup>	H→L	0.7109
	$S_0 \rightarrow T_2$	1.93 eV (nm)	0.0000	H-1→L	0.6787
	$S_0 \rightarrow T_3$	2.01eV (nm)	0.0000	H-2→L	0.6778

<sup>a</sup> Only selected excited states were considered. The numbers in parentheses are the excitation energy in wavelength. <sup>b</sup> Oscillator strength. <sup>c</sup> H stands for HOMO and L stands for LUMO. Only the main configurations are presented. <sup>d</sup> Coefficient of the wave function for each excitations. The CI coefficients are in absolute values. <sup>e</sup> No spin-orbital coupling effect was considered, thus the  $f$  values are zero.

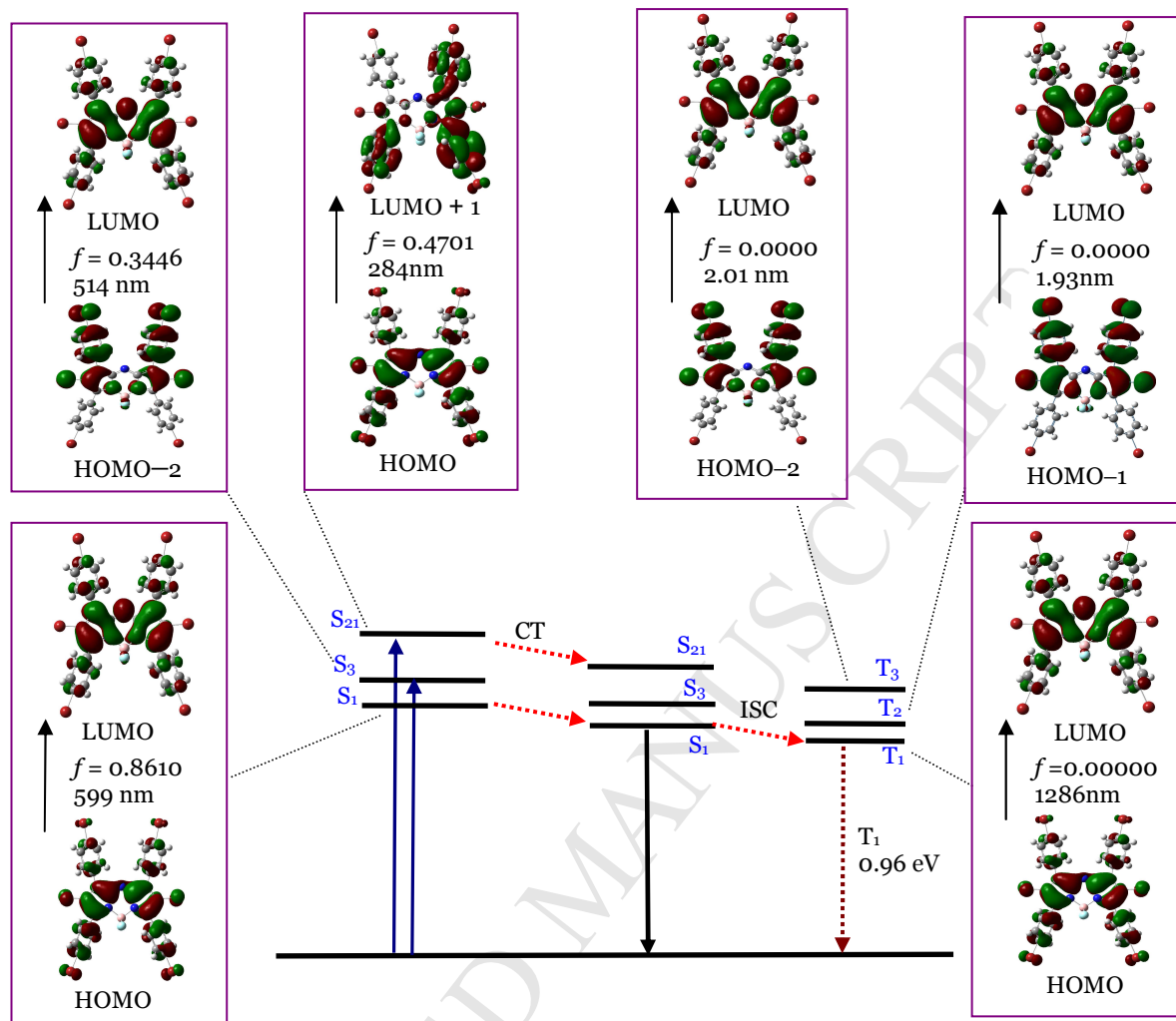


**Figure S29.** Selected frontier molecular orbitals involved in the excitation, emission and triplet excited states of **5d**. CT stands for conformation transformation. The calculations are at the B3LYP/6-31G(d)/LANL2DZ level using Gaussian 09W.

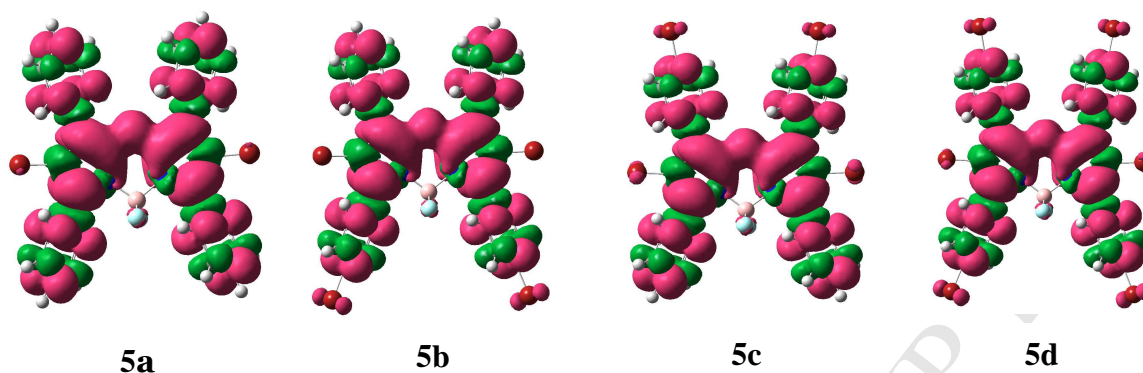


**Figure S30.** Spin density of the complexes **5a**, **5b**, **5c**, and **5d**. Calculated based on the optimized triplet state by DFT at the B3LYP/GENECP/LanL2DZ level by using Gaussian 09W.

#### 4. TWO PHOTON ABSORPTION

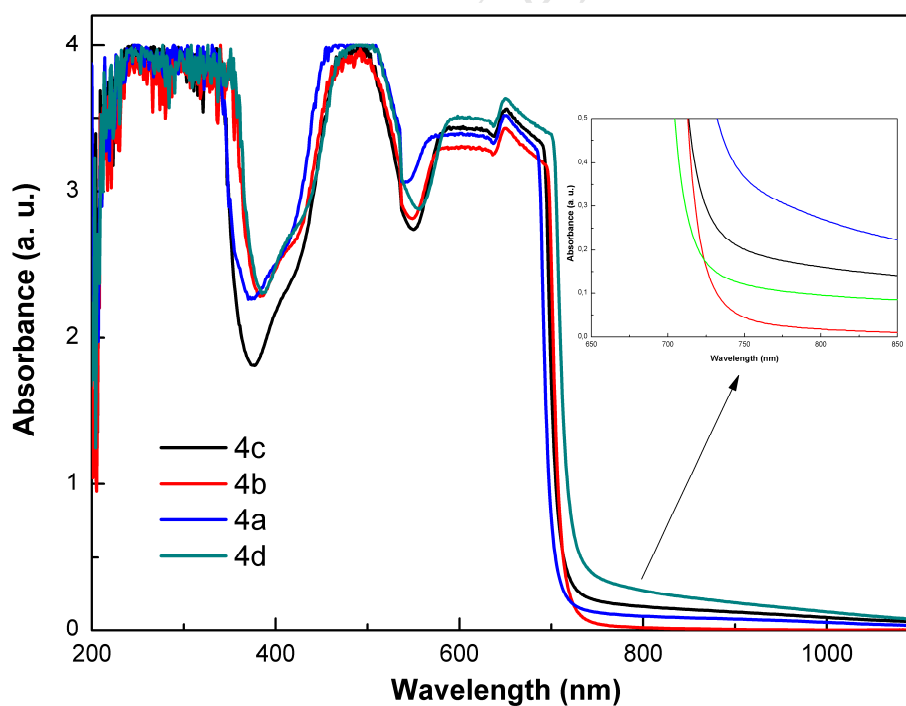


**Figure S31.** Absorption spectra of 4a-d compounds at 0.005 M in THF.

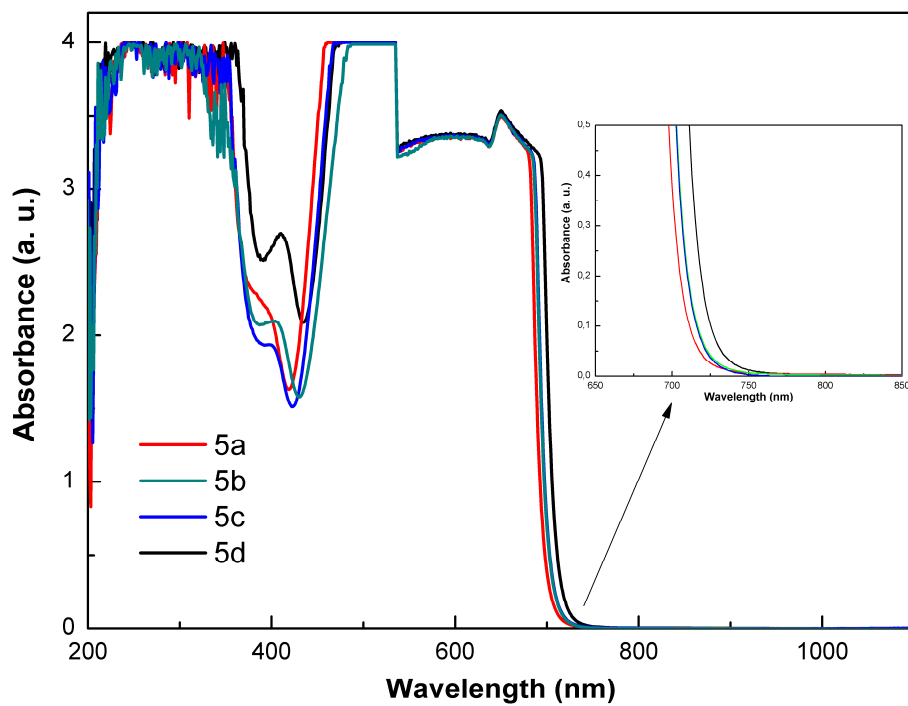


**Figure S32.** Absorption spectra of 5a-d compounds at 0.005 M in THF.

## REFERENCES

- (S1) Bellier, Q.; Pe'gaz, S.; Aronica, C.; Le Guennic, B.; Andraud, C.; and Maury, O. *Org. Lett.* **2011**, 13, 22-25.
- (S2) Gao, L.; Deligonul, N.; Gray, G. T. *Inorg. Chem.* **2012**, 51, 7682–7688.
- (S3) Gorman, A.; Killoran, J.; O'Shea, C.; Kenna, T.; Gallagher, M. W.; O'Shea, D. F. *J. Am. Chem. Soc.* **2004**, 126, 10619-10631.